Heliyon 11 (2025) e42319

Contents lists available at ScienceDirect

Heliyon

journal homepage: www.cell.com/heliyon

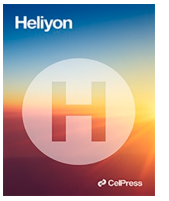

Research article

Examine the impact of green-synthesized nanomaterials on the germination rates and seedling characteristics of African Marigold (*Tagetes erecta* L. var. Pusa Narangi Ganda and Pusa Basanti Ganda)

Kunal Adhikary [a,*], Tapas Mondal [b], Jayoti Majumder [b], Tapas Kumar Chowdhuri [b], Subhra Mukherjee [c], Karishma Maherukh [b]

[a] *Department of Horticulture, School of Agriculture, GD Goenka University, GD Goenka Educational City, Sohna - Gurgaon Rd, Sohna, Sohna Rural, Haryana, 122103, India*

[b] *Department of Floriculture and Landscaping, Bidhan Chandra Krishi Viswavidyalaya, P.O.-Krishi Viswavidyalaya, Mohanpur, Dist.- Nadia, West Bengal, PIN-741252, India*

[c] *Department of Genetics and Plant Breeding, Bidhan Chandra Krishi Viswavidyalay, Mohanpur, Nadia, W.B., PIN-741252, India*

A R T I C L E I N F O

Keywords:
Green synthesis
Germination
Marigold
Nanoparticles
Seedling vigour

A B S T R A C T

Background: West Bengal is key to India's flower industry, contributing 10.61 % of total production, with marigolds valued at 63.44 thousand tonnes. To achieve good yields, many farmers heavily use chemical fertilizers and insecticides. Marigold seeds typically germinate in about 14 days, but farmers often face issues with uneven germination and poor seedling quality.

Materials and methods: This study was conducted at ICAR-AICRP on Floriculture and Landscape Architecture, HRS, Mandouri, Bidhan Chandra Krishi Vishwavidyalaya, West Bengal, India. We synthesized nanoparticles from Tulsi, Doob grass, and Hibiscus extracts in the lab and analyzed them using XRD, SEM, FTIR, and DLS-Zeta methods. We prepared different concentrations of TiO_2 NP, SiO_2 NP, and AgNPs to test their effects on two marigold varieties: Pusa Basanti Ganda and Pusa Narangi Ganda.

Findings: Recent trial results showed that treatments T_4 and T_5 achieved the highest germination percentages, between 90.33 % and 96.67 %, due to increased titanium dioxide nanoparticles (TiO_2 NP). The Vigor Index (VI) was lowest in T_{10} with silver nanoparticles at 521.67, compared to 609.33 for the control group (T_0) in Pusa Basanti Ganda. Seeds treated with silver NPs had longer germination times of 4.5–6.4 days, while silica nanoparticles (SiO_2 NP) had mean germination times ranging from 4.6 to 5.2 days. The root/shoot ratio positively correlated with shoot dry weight (0.501 at $p = 0.05$). In Pusa Basanti Ganda, final germination percentage correlated positively with the Germination Rate Index (GRI), Mean Germination Rate (MGR), and Coefficient of Variation (COV) at values of 0.866, 0.756, and 0.743 respectively, all significant at $p = 0.01$.

Conclusion: The experiment showed that titanium dioxide (TiO_2) nanoparticles at high concentrations enhance seed germination, while silver nanoparticles (AgNPs) hinder it. Silicon dioxide

* Corresponding author.
E-mail addresses: adhikarykunal102@gmail.com, kunal.adhikary@gdgu.org (K. Adhikary), mondal.tapas@bckv.edu.in (T. Mondal), majumder.jayoti@bckv.edu.in (J. Majumder), chowdhuri.tapas@bckv.edu.in (T.K. Chowdhuri).

https://doi.org/10.1016/j.heliyon.2025.e42319
Received 23 May 2024; Received in revised form 21 January 2025; Accepted 27 January 2025
Available online 28 January 2025

(SiO_2) NPs at moderate concentrations support seedling growth. Tested salts at specific concentrations can be recommended to farmers for better crop production.

Abbreviations

TiO_2 NP – Titanium Dioxide Nanoparticles
SiO_2 NPs- Silica Nanoparticles
AgNPs – Silver Nanoparticles
GRI - Germination Rate Index
MGR - Mean Germination Rate
COV - Coefficient of Variation
SiNPs - Silica nanoparticles
ANOVA - Analyses of variance
XRD - X-ray diffraction
SEM - Scanning Electron Microscopy
DLS - Dynamic light scattering
FT-IR - Fourier-transform infrared
T Treatment
Conc. – Concentration

1. Introduction

Nanotechnology involves the manufacturing, characterization, exploration, and application of nanoscale materials (ranging from 1 to 100 nm) for scientific advancement. According to Kaushik et al. [1], nanoparticles act as a bridge between bulk materials and atomic or molecular structures. This field focuses on extremely small structures, with the prefix "nano" deriving from a Greek term meaning "dwarf" or "miniature." By manipulating materials at this scale, nanotechnology enables the engineering of various material properties, leading to research into a wide range of potential applications for nanomaterials. Some of the sectors where nanotechnology has made a significant impact include cosmetics, drug delivery, environmental health, food, healthcare, catalysis, and mechanical engineering [2–4]. Due to their small size, large surface area with loose connections, and higher reactivity compared to their bulk counterparts, they exhibit exceptional and intriguing characteristics [5,6].

Agriculture is the primary source of livelihood for the majority of people in India. Conventional floriculture typically involves the cultivation of plants along with protective measures, which often include the use of chemical fertilizers, pesticides, and other industrial products to increase crop yields. However, in recent years, nanotechnology has garnered greater interest in the horticulture sector

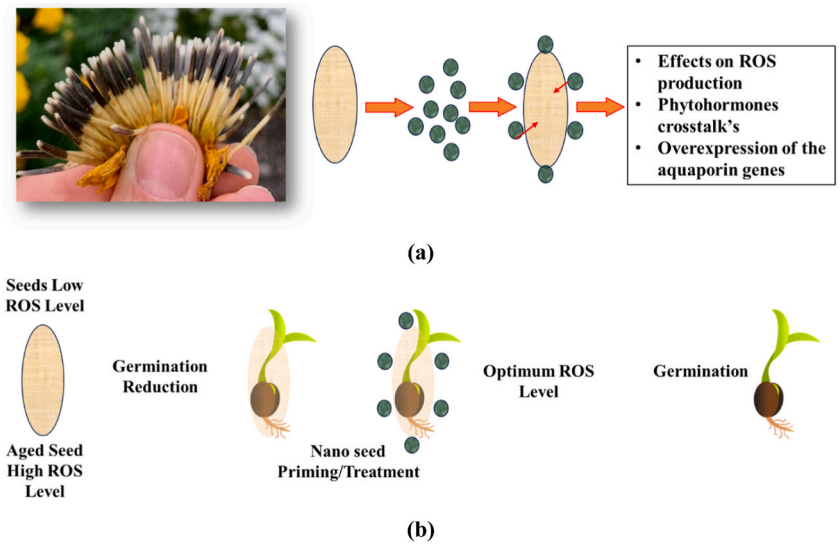

Fig. 1. (a) Diagrammatical representation of the effects of nanoparticle seed priming (b) Role of nanoparticles in ROS level optimization.

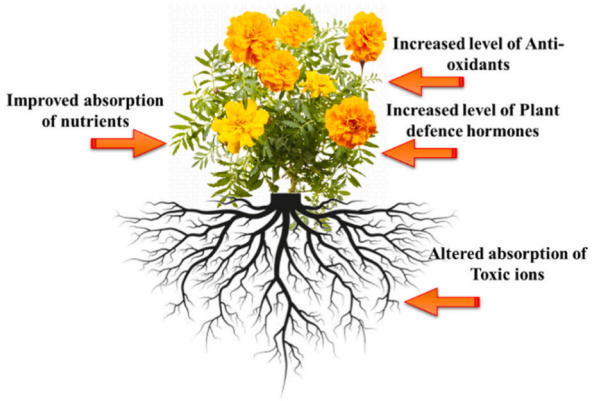

Fig. 2. Effects of nanoparticles on the plant after the seed treatment with NPs.

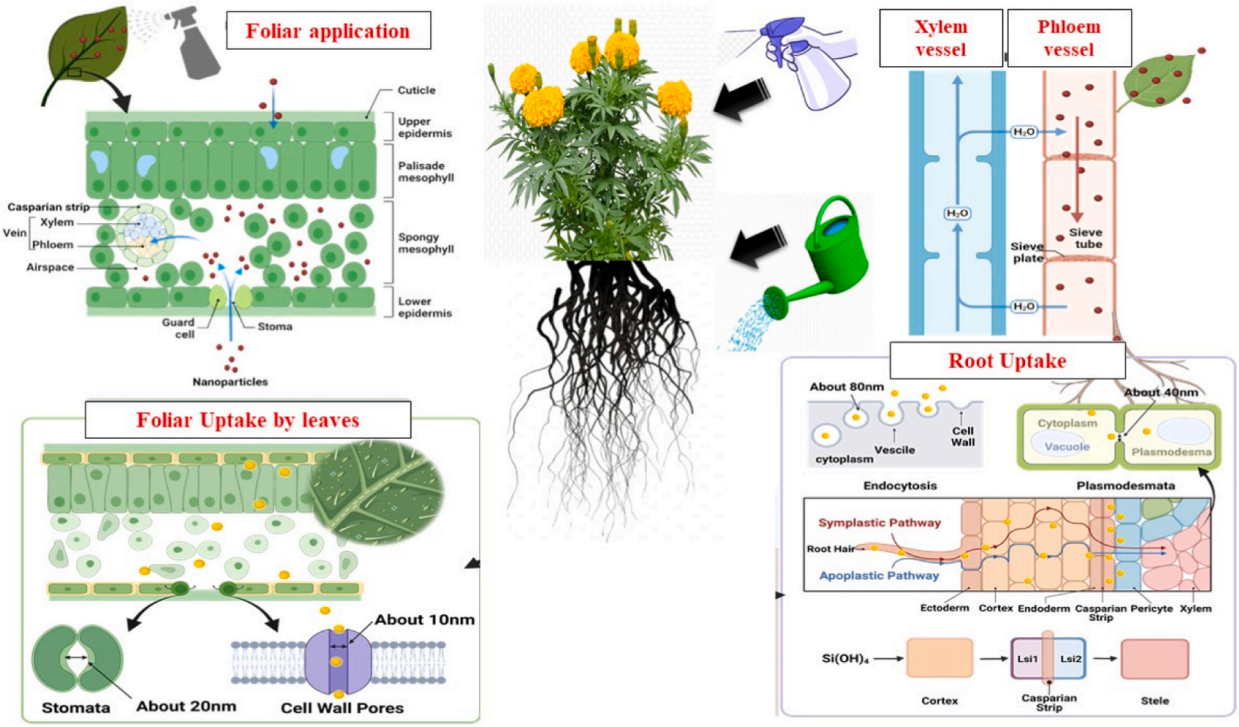

Fig. 3. Absorption and Translocation pathway of Nanoparticles Created in Biorender

compared to these traditional practices [7,8]. By utilizing eco-friendly nanoparticles, it is possible to enhance the effectiveness of agricultural chemicals while using lower dosages. Agricultural nanotechnology and its associated techniques can significantly improve flower crop yields and reduce the impact of diseases on plants (Fig. 2.). Nanoparticles have demonstrated a significant impact on various cellular processes in plants, encompassing sensing, signaling, transcription, transcript processing, translation, and post-translational protein modifications [9]. These nanoparticles have the capacity to activate specific signaling pathways that play essential roles in stress responses, nutrient uptake, and hormone signaling [10]. For instance, studies indicate that nanoparticles can promote the expression of stress-responsive genes, engage defense mechanisms against pathogenic threats, and enhance the uptake of vital nutrients. Consequently, these effects contribute to the overall health and performance of plants [11].

The green synthesis technique utilizes plant extracts as stabilizing and reducing agents instead of harmful chemicals, making it an environmentally sustainable alternative to traditional chemical processes [12–14]. This method promotes overall sustainability by using renewable resources, operating under ambient conditions, having a minimal environmental impact, and conserving energy. Additionally, biodegradable materials derived from plants are used in the synthesis, ensuring safe disposal and reducing long-term environmental effects [15]. Green synthesis is based on the sensible use of non-polluting chemicals to synthesize nanomaterials, as

well as the use of healthy solvents such as water and natural extracts. Major metabolites in plants, such as reducing sugars, proteins, peptides, and so on, play an explanatory role in the stability and reduction of NPs. Park et al. [16] studied the role of polysaccharides in gold and AgNPs synthesis, and beta D-glucose was used as a reducing agent and starch as a stabilizer in AgNPs synthesis [17].

The potential of active nanoparticles or nanocarrier systems to boost seed germination can be explained by the fact that nanoparticles may penetrate the seed coat at ideal concentrations, increasing the number of holes in the coat and, as a result, increasing water uptake and oxygen transfer (Fig. 1a) [18]. The absorption of nanoparticles under seed coating can stimulate ROS production by acting in various metabolic pathways, increasing the number of active gibberellins, and mobilizing storage proteins [19]. Furthermore, the influence of nanoparticles on seed water intake can produce enough stress to start germination, increasing the activity of enzymes in stages I and II of the process. Joshi et al. [20], reported that seed nano-priming has been found to improve germination because these systems can keep ROS levels within the ideal range defined by the oxidative window that promotes seed germination (Figs. 1b & 2).

The unique features and advantages of silica nanoparticles (SiNPs) include their nanoscale sizes, nutritional effects, surface properties, and porous nature. These characteristics enable them to serve various functions in nano-enabled agriculture, such as acting as plant growth stimulators, nanocarriers, and soil conditioners [21,22]. Numerous laboratory and field studies have demonstrated that SiNPs, when used as plant growth stimulators, can enhance plants' resistance to a range of biotic stresses (such as insect pests and pathogens) and abiotic stresses (such as metal stress, drought stress, and salt stress). This leads to improved plant growth, yield, and quality [23–25]. Furthermore, the porous nature of SiNPs makes them ideal carriers for delivering various chemicals (including fertilizers, pesticides, and plant growth regulators) and bioactive molecules (such as DNA and proteins) in agricultural production and plant biotechnology [26,27].

Titanium dioxide nanoparticles (TiO_2-NPs) are rapidly becoming a focal point of research and application due to their remarkable versatility. They possess a wide array of beneficial properties, including antibacterial, antifungal, antiviral, anticancer, and antioxidative effects, making them invaluable in pharmaceuticals and other medicinal fields [28]. For instance, research by Andersen et al. [29] revealed that the application of TiO2-NPs to Brassica oleracea significantly boosted plant growth and yield. Moreover, in *Ocimum basilicum*, TiO2-NPs enhanced seed germination by promoting the formation of both the plumule and radicle [30]. Notably, even single-generation exposure to nano-TiO2 can positively modulate key plant processes, including germination, seedling growth, photosynthesis, metabolism, antioxidant defense, and overall yield [31–33]. Clearly, TiO2-NPs represent a powerful tool in advancing agricultural productivity and improving plant health.

Research shows that plants possess a remarkable ability to absorb, translocate, and accumulate silver nanoparticles (AgNPs) from their surroundings [34] (Fig. 3.). This swift absorption process occurs more rapidly than the dissolution of these nanoparticles in the soil, highlighting an efficient uptake mechanism. Noble metals like gold, platinum, silver, titanium, and palladium are extensively utilized in synthesizing nanomaterials. However, silver nanoparticles stand out for their exceptional properties, including intricate surface morphology, precise size distribution, diverse particle composition, and high reactivity in solution. Their effectiveness in ion release, coupled with notable electronic, thermal, optical, magnetic, and catalytic features, underscores their growing importance in various applications [35,36]. Silver nanoparticles (AgNPs) synthesized from *Moringa oleifera* leaf extract have proven to be highly effective in enhancing seed germination and growth. In a controlled study, various concentrations of AgNPs—25 ppm, 50 ppm, 75 ppm, and 100 ppm—were evaluated to determine their impact on wheat seeds. Impressively, the 100-ppm concentration exhibited remarkable growth compared to the control group. This concentration also led to significant increases in dry root weight, fresh root weight, root elongation, and root length, showcasing the potential of AgNPs as a powerful agent for improving agricultural productivity and crop health [37,38].

Marigold (*Tagetes erecta* L.) is a vibrant member of the Asteraceae family, thriving in the rich soils of Central and South America, especially Mexico. This stunning flower is not only a beloved ornamental choice but also stands as a cornerstone in the global floriculture industry. According to the National Horticulture Board's (NHB) [39] advance estimates for 2023-24, India is poised to produce an impressive 2,284,000 tonnes of loose marigold flowers and 947,000 tonnes of cut flowers. The nation dedicates 285,000 ha to floriculture production, showcasing its commitment to this thriving sector. In India, West Bengal shines brightly, contributing 10.61 % to the commercial floriculture landscape. With marigold production valued at 63.44 thousand tonnes in the state, it's clear that investing in this colourful flower not only beautifies our surroundings but also fuels economic growth and agricultural prosperity.

During discussions with farmers, it has been observed that both qualitative and quantitative yield are major concerns. To achieve good yields, farmers often rely on the excessive use of chemical fertilizers and insecticides. Germination of marigold seeds takes approximately 14 days [40], depending on agro-climatic conditions. However, farmers sometimes face issues with uneven germination and poor quality of seedlings. The primary objective of this research was to investigate the impact of plant-mediated nanoparticles on the germination rates and seedling characteristics of two prominent cultivars of African marigold: Pusa Narangi Ganda and Pusa Basanti Ganda. This study was conducted in the Nadia district of West Bengal, an area known for its floricultural practices. Furthermore, the research focused on standardizing the appropriate dosage of green-synthesized nanomaterials to be used as a seed treatment specifically for marigold plants. The findings of this study aim to provide valuable recommendations for farmers, enhancing their cultivation techniques and potentially improving crop yields.

2. Materials and methods

2.1. Green synthesis of silver nano particles using Ocimum tenuiflorum

Healthy leaves of *Ocimum tenuiflorum* were collected from areas surrounding Bidhan Chandra Krishi Vishwavidyalaya, Bardhhaman Campus, Bardhhaman, West Bengal (23.2408° N, 87.8955° E). The freshly harvested leaves underwent a washing process of 2–3

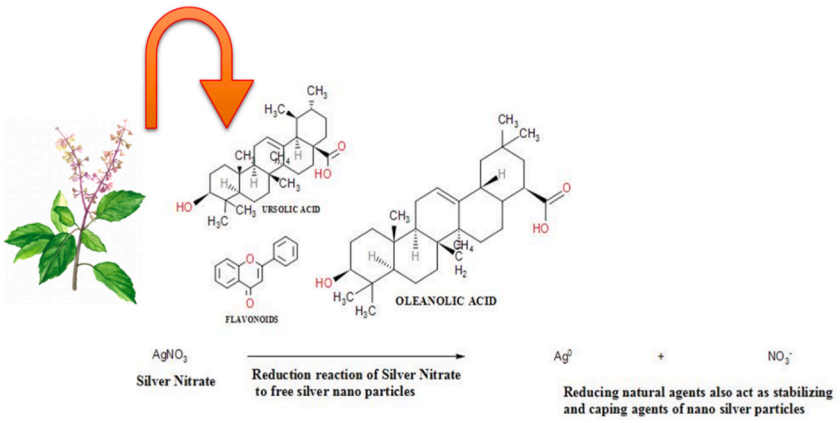

Fig. 4. Flowchart for the Process of Synthesizing Silver Nanoparticles Using Extract from *Ocimum tenuiflorum*. This scheme outlines the chemical reactions involved in the reduction of silver ions to form silver nanoparticles with the help of phytochemicals present in *Ocimum tenuiflorum*, commonly known as holy basil. Created in KingDraw and MS Office.

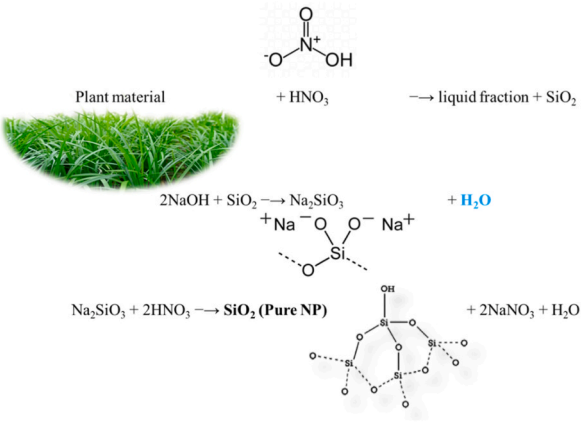

Fig. 5. The schematic provides a detailed illustration of the chemical reaction that leads to the synthesis of silicon dioxide (SiO_2) nanoparticles utilizing an extract from the plant *C. dactylon*. This process highlights the interaction between the extract and the precursor materials, showcasing how the nanoparticles are formed. Created in KingDraw and MS Office.

times under running water and were subsequently dried in the shade for a maximum duration of 10 days under germ-free conditions. A total of 25 g of basil leaves were thoroughly washed in distilled water (3–4 times), dried, chopped, and ground in 100 mL of sterile distilled water. This mixture was filtered using Whatman filter paper No. 45 μm, and the resultant extract was stored at 4 °C for subsequent testing [41,42]. An aqueous solution of 1 mM silver nitrate ($AgNO_3$) was prepared to facilitate the synthesis of silver nanoparticles. To this solution, 10 mL of the *Ocimum tenuiflorum* extract were added to 90 mL of the 1 mM silver nitrate solution, allowing for the reduction of Ag + ions. The mixture was kept at room temperature for a duration of 15 h (Fig. 4). In this context, the filtrate functions as a reducing agent and stabilizer for the silver nanoparticles formed from the $AgNO_3$ solution [43,44].

2.2. Green synthesis of SiO_2 nano particles using Cynodon dactylon

Freshly harvested leaves of *Cynodon dactylon* were collected, subsequently washed 2 to 3 times under running water, and dried in the shade for a duration of up to 10 days under germ-free conditions. The dried leaves were then ground thoroughly using a kitchen blender and subjected to sieving through a 5 mm sieve plate to facilitate the synthesis of silicon dioxide nanoparticles (SiO_2NPs) [45–47]. A total of 25 g of the well-ground leaf powder was combined with 500 mL of 1 M nitric acid (HNO_3) in a 1000 mL conical flask and stirred for 6–7 h. The resultant mixture was filtered and subsequently washed with distilled water to adjust the pH to a range of 4.0–5.0. The solution was then dried in an oven at a temperature between 100 °C and 110 °C for 12 h. The resulting turbid solution was mixed with 500 mL of 1 M sodium hydroxide (NaOH) and stirred for 6–7 h using a magnetic stirrer to elevate the pH to 12. Following this process, the reaction mixture was separated via a suction pump and titrated with 3 M nitric acid (HNO_3) until the pH was adjusted to between 8.5 and 9.0. The components were then centrifuged at 5000 rpm for 10 min to isolate the biological mixture. The collected contents were washed 3 to 4 times with distilled water and subsequently dried at 80 °C in a hot air oven for a period of 12 h. The

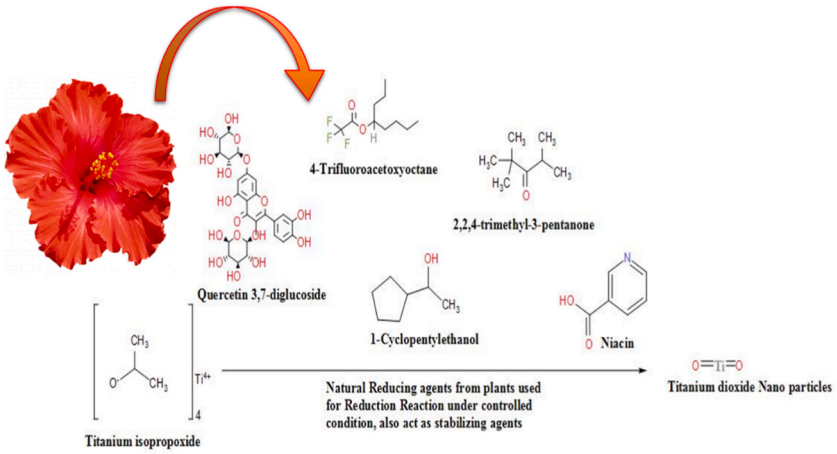

Fig. 6. Detailed Scheme of the Chemical Reaction for the Synthesis of Titanium Dioxide Nanoparticles Utilizing Extracts from *Hibiscus rosa-sinensis*. This process involves the extraction of natural compounds from Hibiscus rosa-sinensis, which serve as precursors in the formation of titanium dioxide nanoparticles through a series of chemical reactions. Created in KingDraw and MS Office.

resulting powder was finely ground with a mortar and pestle for further characterization (Fig. 5.). The liquid phase was removed, and the silicon dioxide pellet was washed multiple times with distilled water. The solid contents were then stirred with 1 M sodium hydroxide to produce sodium silicate and water molecules. This mixture was pumped and titrated with 3 M nitric acid to achieve the pure form of silicon dioxide, sodium nitrate, and water. Notably, as the 3 M nitric acid solution was added dropwise to the pumped plant mixture, a gradual transition in color was observed, shifting from brown to a white precipitate [48–50].

2.3. Green synthesis of TiO_2 nano particles using Hibiscus rosa sinensis

Healthy leaves of *Hibiscus rosa-sinensis* were collected from the vicinity of Bidhan Chandra Krishi Vishwavidyalaya in Mohanpur, Nadia, West Bengal. The collected fresh leaves were thoroughly washed 2 to 3 times using running tap water and subsequently shade-dried. A quantity of 10 g of air-dried petals was placed into a beaker and extracted with 200 mL of water at a temperature ranging from 70 to 80 °C for a duration of 3 h. The resultant extract was filtered using Whatman filter paper, and the filtrate was stored for the synthesis of nanoparticles [51,52]. For the synthesis of titanium dioxide (TiO_2) nanoparticles, 100 mL of 1.0 N Titanium Isopropoxide (TTIP) was dissolved in distilled water. The flower extract was incorporated dropwise under conditions of constant stirring until the pH of the solution was adjusted to 7. The mixture was stirred continuously for a period of 4–5 h during which time the nanoparticles formed. These nanoparticles were subsequently separated using filter paper and washed with water to eliminate any by-products. Finally, the nanoparticles were dried at a temperature of 80–90 °C for 12 h. The resulting powder was meticulously ground using a mortar and pestle and prepared for characterization (Fig. 6) [53–55].

2.4. Characterisation of nanoparticles

Results from Fourier Transform Infrared Spectroscopy (FT-IR), X-ray Diffraction (XRD), Scanning Electron Microscopy (SEM), Energy Dispersive X-ray Spectroscopy (EDAX), and Dynamic Light Scattering (DLS) were utilized to characterize the synthesized green-based nanoparticles [56–58]. The size of the nanoparticle crystals was measured using a BRUKER X-Ray Diffractometer located at the CIF, IACS, Jadavpur, Kolkata. This instrument operates at 30 kV and 40 mA, with a 2θ range of copper ranging from 10.0° to 89.9°. The FT-IR spectrum was captured with a PERKIN ELMER FT-IR spectrometer, which operates at a resolution of 4 cm^{-1}, incorporating KBr optics that offer a resolution of 0.5 cm^{-1} over a range of 8300–350 cm^{-1} [59]. For the analysis of sample morphology, a field emission scanning electron microscope ('JEOL') was employed to obtain SEM images. Both SEM and EDAX techniques were used to assess the size, shape, and elemental composition of the nanoparticles. Additionally, this study analyzed the average size and zeta potential of the colloidal solution of metal nanoparticles using the MALVERN Particle Size and Zeta Potential Analyzer [60–62].

2.5. Experimental details

The study was carried out as a test for germination and seedling health, where seeds were subjected to green synthesized nanomaterials at different concentrations, as outlined in Table 1. Subsequently, the growth parameters of the seeds and seedlings were assessed based on a Complete Randomized Design (CRD) [63,64]. This study took place in a laboratory setting under controlled conditions at room temperature using petri dishes [65]. The seeds were thoroughly rinsed and then sun-dried, with a selection of 25 healthy seeds gathered from each variety. The seeds were evenly distributed over the petri dishes lined with filter paper, after which the prepared nanoparticle solution was evenly applied for observation.

Table 1
Treatments and experimental details.

Treatment		Concentration (ppm)
Nano materials	T_0	0
TiO_2 (Titanium oxide Nano particles)	T_1	20
	T_2	40
	T_3	60
	T_4	80
	T_5	100
Ag NP (Silver)	T_6	5
	T_7	10
	T_8	20
	T_9	40
	T_{10}	60
SiO_2 (Silica Nano particles)	T_{11}	5
	T_{12}	10
	T_{13}	15
	T_{14}	20
	T_{15}	50
Design of experiment		CRD
No of treatment		16
No of replication		3
No of seeds per Petri plate		25
Plant/pot		1
Variety		Pusa Basanti Ganda Pusa Narangi Ganda

2.6. Observation recorded

Seeds of African marigold was subjected to treatments with different concentrations of green synthesized nanoparticles in a controlled environment. Observations were conducted on a daily basis, following the methodology outlined by El-Kassaby et al. [66]. During this process, we meticulously recorded all essential parameters related to germination and seedling development. These parameters included germination rate, root length, shoot height, and overall seedling vigor, among others. The observed parameters are presented in Table 2. This study aims to enhance our understanding of how these nanoparticles influence the growth and development of this important ornamental plant.

2.7. Statistical analysis

Observations were recorded daily based on a Completely Randomized Design (CRD) with four replicates and 15 treatments under controlled conditions. The statistical analysis of the experimental results was conducted using R Studio software (version 4.3.1) [67], Origin Pro, and Microsoft Excel Office 2021. To evaluate the significance of the concentration of dressing agents on seed germination percentage and seedling parameters, both intragroup and intergroup analyses of variance (ANOVA) were performed. Significant differences were assessed using a general linear model, and means were compared using Student's t-test at a 5 % probability level ($p \leq 0.05$) [68].

3. Result and discussion

3.1. Characterization of AgNPs synthesized from Tulsi extract

3.1.1. FT-IR spectra of silver nanoparticles (AgNPs)

Fig. 8a showcases sharp FT-IR spectra of silver nanoparticles (AgNPs), featuring distinct absorption peaks at approximately 671.52 cm^{-1}, 1415.31 cm^{-1}, 1642.41 cm^{-1}, and 3426.02 cm^{-1}. The peak at 671.52 cm^{-1} indicates C-Cl stretching from halides, while 1415.31 cm^{-1} corresponds to C-O stretching in alcohols and phenols (Table 3). The peak at 1642.41 cm^{-1} is associated with C=O stretching typical of tertiary amides, and the strong peak at 3426.02 cm^{-1} represents O-H stretching from alcohols and phenols. These observations suggest that carbonyl groups from amino acids and proteins effectively bind to metal ions, forming stable complexes. This interaction may also facilitate the formation of a biomolecular layer around the AgNPs, enhancing their stability and potential applications [62,76,77]. The absorption spectrum near 1415 cm^{-1} corresponds to the stretching vibration of the carbon-carbon double bond (-C=C-). A peak around 1239 cm^{-1} indicates the presence of amide I bonds, which are essential in protein structure. Functional groups like -C-O-C-, -C-O-, and -C=C- are commonly found in heterocyclic compounds. Notably, the amide I bonds from proteins serve as vital capping ligands for nanoparticles, playing a key role in stabilizing and functionalizing these materials for various applications [78,79].

Table 2
Germination and seedling parameters.

Parameters	Formulae	Description	Note and references
Coefficient of velocity of germination (CVG)	$Coefficient\ of\ Velocity\ of\ Germination\ (CVG) = \frac{\sum Ni}{\sum NiTi} \times 100$	Ni = Number of germinated seeds per day, Ti = Number of days from the start of the count (the number corresponding to the i th interval)	The coefficient of variation for germination (CVG) serves as an important indicator of the speed of seed germination. It increases when the number of germinated seeds rises and when the time required for germination decreases. Theoretically, the highest possible CVG is 100, which would occur if all seeds germinated within the first day [69].
Germination Rate or Germination Rate Index (GRI)	$Germination\ Rate\ or\ Germination\ Rate\ Index = \sum GT/Tt\ or \left[\frac{Number\ of\ germinated\ seed}{Days\ of\ first\ count}\right] + \ldots\ldots\ldots \left[\frac{Number\ of\ germinated\ seed}{Days\ of\ last\ count}\right]$		The germination rate is defined as the percentage of seeds that successfully germinate within a specified time period. This metric is essential for assessing seed viability and overall agricultural performance.
Mean Germination Time	$Mean\ Germination\ Time\ (MGT) = \frac{\sum NiTi}{\sum Ni}$		Mean Germination Time (MGT) represents the average duration required for the maximum germination of a seed lot. It is calculated as the reciprocal of the mean germination rate [70]. Consequently, a lower MGT signifies a more rapid germination process within a population of seeds.
Mean Germination Rate	$Mean\ Germination\ Rate\ (MGR) = \frac{\sum Ni}{\sum NiTi}$		Mean germination rate (MGR) is a measurement that indicates how quickly seeds germinate over a unit of time. It is calculated as the reciprocal of the mean germination time (MGT) [71].
Final Germination %	$Final\ Germination\ \% = \frac{Number\ of\ Total\ Seed\ Germinated}{Total\ Number\ of\ Seed\ Tested} \times 100$		Germination percentage (GP) is an important metric that assesses the viability of seeds within a given population. This percentage is determined by dividing the number of seeds that successfully germinate by the total number of seeds sown [72].
Vigour Index	$Seedling\ Vigour\ Index\ (SVI) = Seedling\ length \times Germination\ \%$		Seed vigor is a vital indicator of seed quality and is used to assess a seed's potential for growth and crop production. Seeds with high vigor are more likely to thrive in various field conditions [73].
Seedling parameters	Shoot length (cm.), Root length(cm.), Total Length(cm.), Root fresh weight(g.), shoot fresh weight(g.), Root/shoot fresh weight, Root dry weight(g.), Shoot dry weight(g.), Root/shoot dry weight	Seedling attributes such as shoot length, root length, and root-shoot fresh and dry weight are key parameters for assessing seedling health and growth index.	[74,75]

Table 3
FTIR spectral characteristics of AgNPs synthesized from Tulsi extract.

Peak Number	X (cm^{-1})	Functional group
1	3426 cm^{-1}	–OH, Characteristic of carbohydrate monomers including mannose and uronic acid at 3430 cm^{-1} showed a slight shift
2	2916 cm^{-1}	C–H Symmetrical and asymmetrical C–H stretching of aliphatic –CH and –CH2 groups
3	1743 cm^{-1}	C = O 1743 cm^{-1} is characteristic of C = O stretching, indicating the presence of carbonyl groups in Tusi.
4	1239 cm^{-1}	C–O–C stretching of –COCH3 groups
5	1075 cm^{-1}	C–O stretching associated with rhamnogalacturonan, a side-chain constituent of pectins

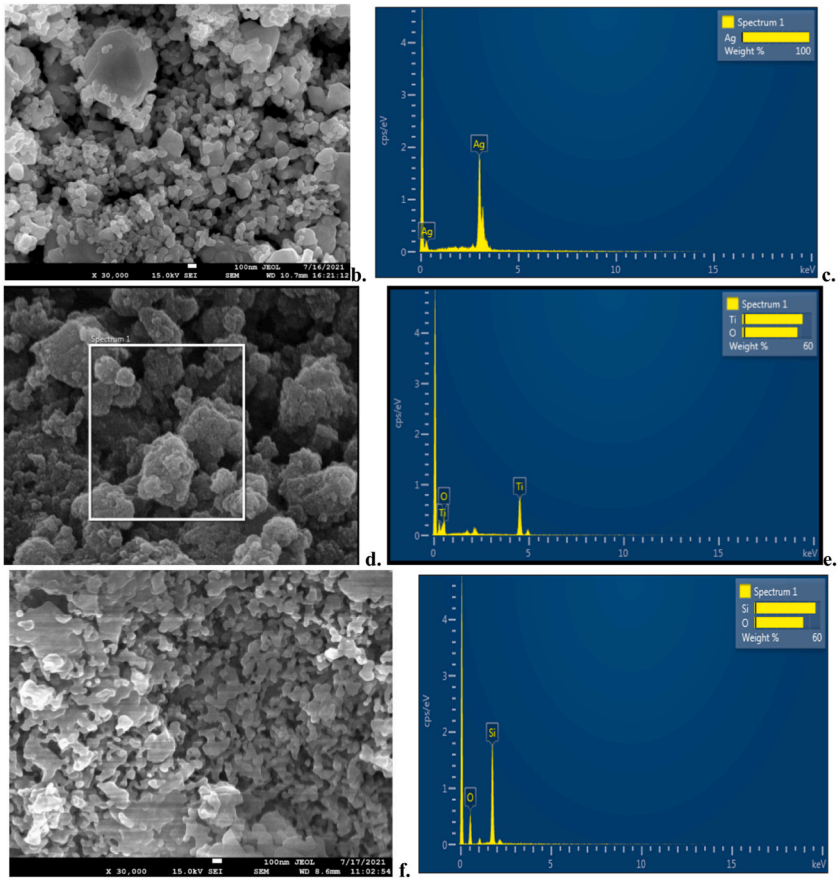

Fig. 7. SEM and EDS of Plant-mediated nano particles: AgNPs (a, b); TiO_2 NPs (c, d); SiO_2 NPs (e, f).

3.1.2. XRD pattern of AgNPs

The X-ray diffraction (XRD) pattern of silver nanoparticles (AgNPs) synthesized using Tulsi leaf extract is presented in Fig. 9a. XRD analysis was conducted to assess the crystallinity of the AgNPs. Significant peaks were observed at angles of 38.43°, 45.05°, 67.25°, and 79.30°, correlating with the (112), (202), (222), and (322) planes. These results were compared with the standard powder diffraction pattern from the Joint Committee on Powder Diffraction Standards (JCPDS), specifically Silver File No. 04–0783, which confirms a face-cantered cubic structure. The characteristic peaks observed at 27.27, 31.66, and 45.74 provide evidence for the crystalline nature of the bio-organic phase, specifically the capping agent, present on the surface of the silver nanoparticles (Ag NPs) [80]. The Debye-Scherrer formula was utilized to know the average crystallite size (~16 nm–50 nm). These Bragg peaks may be attributed to bio-organic compounds or proteins present in the Tulsi leaf extract, as corroborated by the findings of Aref and Salem, [81].

3.1.3. SEM and EDX analysis of AgNPs

Among the various techniques available in electron microscopy, Scanning Electron Microscopy (SEM) stands out as a surface imaging method that adeptly resolves diverse particle sizes, size distributions, nanomaterial shapes, and the surface morphology of synthesized particles at both micro and nanoscale levels. The SEM images demonstrated that the majority of silver nanoparticles were predominantly spherical, exhibiting smooth surfaces and a well-dispersed arrangement in a dense and compact formation, similar findings were previously reported by Alharbi et al. [83] (Fig. 7a and b). In a study conducted by Hemlata et al. [82], the green synthesis of silver nanoparticles (AgNPs) was achieved using the aqueous leaf extract of *Cucumis prophetarum*. The resulting Cp-AgNPs exhibited a range of polymorphic shapes, with some particles appearing irregularly granulated, ellipsoidal, and highly aggregated. The average size of these nanoparticles was found to range from 30 to 50 nm.

3.1.4. DLS and zeta analysis of AgNPs

To evaluate the particle size distribution, the synthesized green silver nanoparticles (AgNPs) were analyzed using dynamic light scattering (DLS). The results, presented in Fig. 10(a and b), demonstrate that the particles are monodispersed, with an average size of approximately 52.4 nm. The stability of the nanoparticles was examined through zeta potential measurements, as shown in Fig. 12. The zeta potential values were found to be significantly negative, recorded at −6.97 mV, along with a conductivity of 0.139 mS/cm

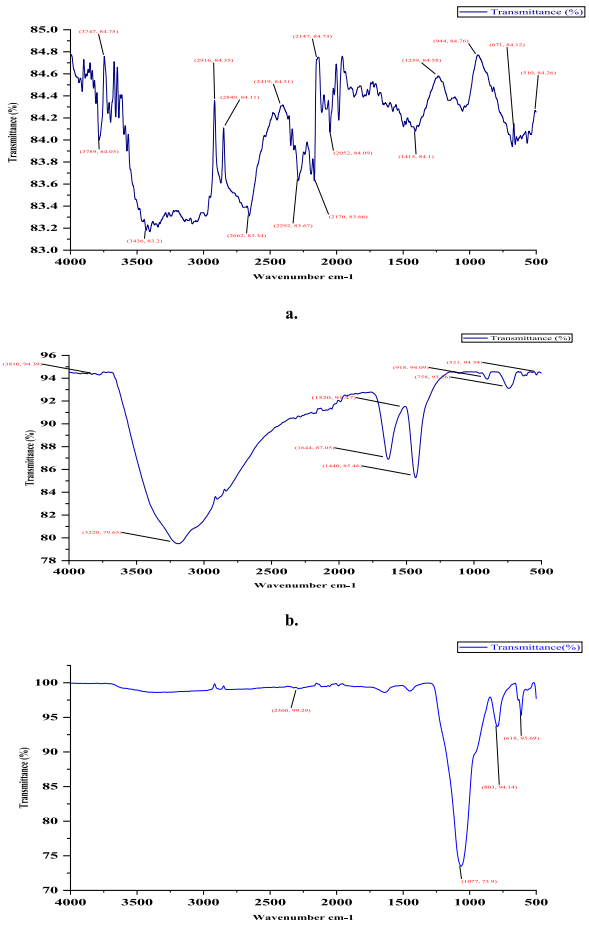

Fig. 8. Fourier-transform infrared spectroscopy (FTIR) of a. AgNPs b. TiO_2 NPs c. SiO_2 NPs (created by Origin Pro).

[80,81,83]. These findings indicate a favourable colloidal stability of the particles. This outcome aligns well with the results reported by Hemlata et al., [82]. Similarly, Felix et al. [84] effectively synthesized silver nanoparticles (AgNPs) through green synthesis method. They accurately assessed the hydrodynamic diameter and zeta potential using dynamic light scattering (DLS). The nanoparticles exhibited an impressive average size of about 83.85 nm, alongside a zeta potential of 43.6 mV, reflecting excellent stability and promising potential for various applications.

3.2. *Characterization of TiO_2 synthesized from Hibiscus flower extract*

3.2.1. *FT-IR spectra of TiO_2NP*

The functional groups and compounds present in the synthesized titanium dioxide (TiO_2) nanoparticles (NPs) were characterized using Fourier-transform infrared (FT-IR) spectroscopy. Fig. 8b illustrates the FT-IR spectrum of plant-derived TiO_2 across a wavenumber range of 400–4000 cm^{-1}. Notable peaks at 3189.08 cm^{-1} and 1634.22 cm^{-1} are attributed to the stretching and bending vibrations of hydroxyl (-OH) groups. In the spectrum of pure TiO_2, the peak at 521.88 cm^{-1} indicates Ti-O stretching, while the peak at 1440 cm^{-1} corresponds to Ti-O-Ti stretching. Furthermore, the peak at 3810 cm^{-1} suggests the presence of amines, the peak at 3287.11 cm^{-1} indicates alkynes, the peak at 3011.35 cm^{-1} is associated with aromatic rings, and the peak at 1712.28 cm^{-1} corresponds to pyridine. The band cantered at 1388 cm1 is assigned to bending vibration of C-H bond in prepared TiO_2 at 400 °C [85,86]. The increase in temperature attributes to the absence of C-H bond at higher temperature. These phytochemicals play a crucial role in the reduction of titanium dioxide to stable TiO_2 during the green synthesis process [51,52,52].

3.2.2. *XRD pattern of TiO_2NP*

The crystalline structure of titanium dioxide (TiO_2) was investigated using powder X-ray diffraction (XRD) analysis. The results indicated the presence of both rutile and anatase phases (Fig. 9b). The observed diffraction peaks were notably broad, suggesting the formation of nanoscale crystals. Specifically, the XRD patterns exhibited distinct peaks at 25.44°, 36.16°, 47.91°, and 54.43°, which are indicative of the anatase phase, corresponding to the (101), (103), (200), and (105) planes, respectively. Furthermore, peaks at 27.47°,

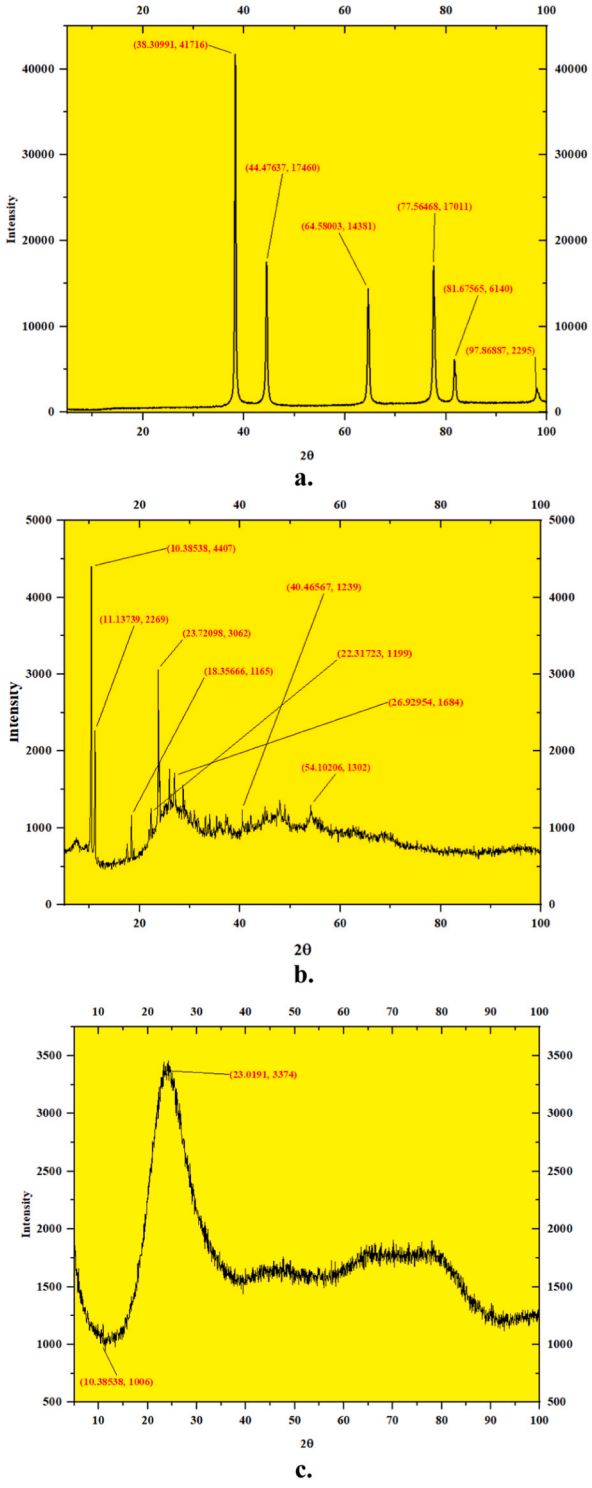

Fig. 9. X-ray diffraction (XRD) of a. AgNPs b. TiO_2 NPs c. SiO_2 NPs (created by Origin Pro).

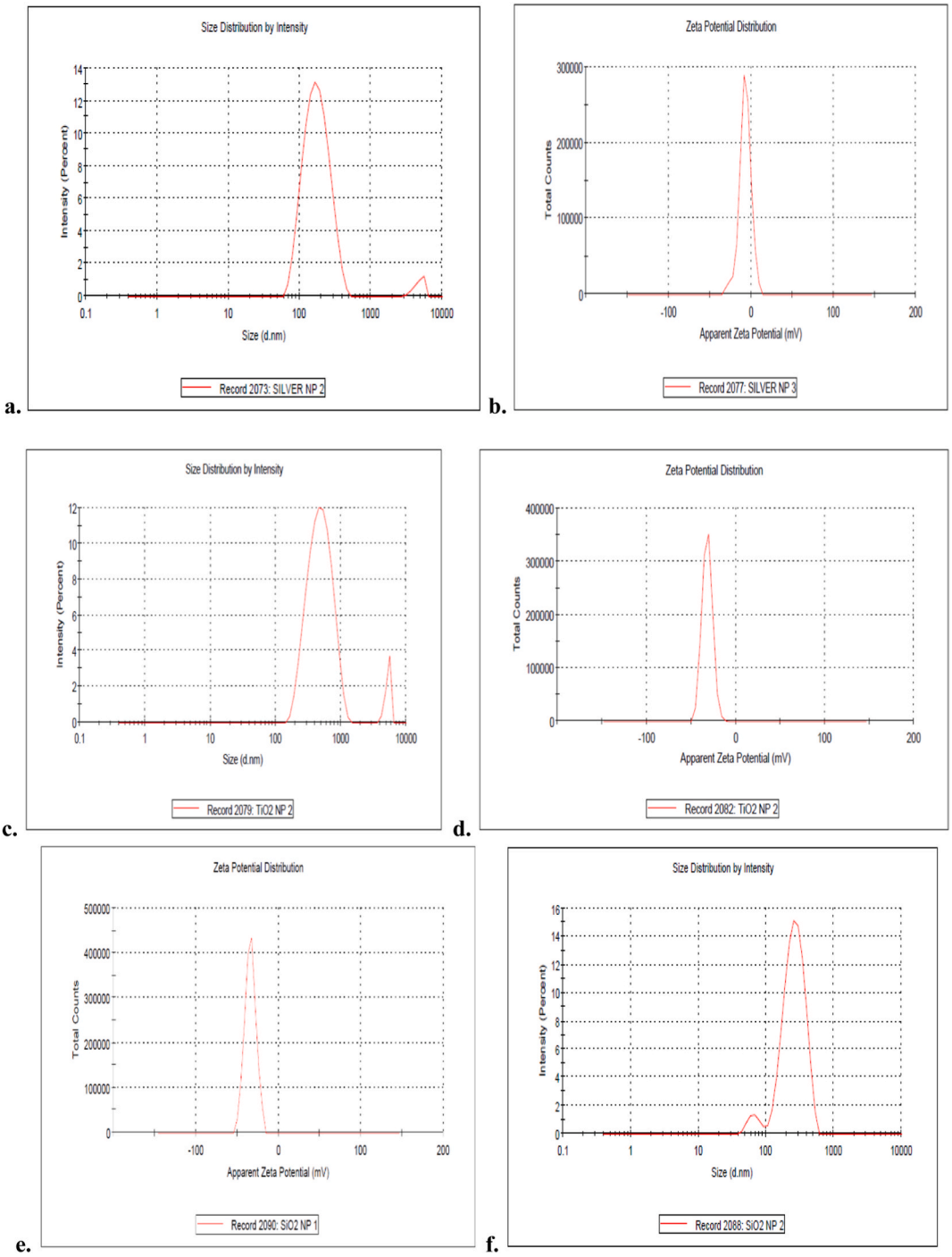

Fig. 10. DLS size and Zeta Potential of Plant-mediated nano particles: AgNPs (a, b); TiO_2 NPs (c, d); SiO_2 NPs (e, f).

41.20°, 56.62°, and 69.35° were identified as representative of the rutile phase, with corresponding planes (110), (111), (220), and (301) Fig. 8b. The average crystal size was estimated to be 30–45 nm, calculated by Scherrer's formula.

$$D = \frac{K\lambda}{\beta \cos\theta}$$

where D is crystalline size, λ is wavelength of X-ray (1.54 Å), β is full width half maxima, θ is Bragg angle, K is shape factor (0.9). The particle size is recognized as a critical factor that significantly affects the properties and applications of nanomaterials. The crystallite

Table 4
Effects of green synthesized nanoparticles on germination attributes of Pusa Narangi Ganda.

	TREATMENT	FINAL GERMINATION %	GERMINATION RATE INDEX (%/day)	MEAN GERMINATION TIME (days)	COEFFICIENT OF VELOCITY	MEAN GERMINATION RATE
	CONTROL	70.12	0.085	6.537	2.420	0.025
TiO_2 NPs	T_1 (20 mg/l)	80.00	0.102	5.537	2.663	0.029
	T_2 (40 mg/l)	83.33	0.102	4.647	2.957	0.031
	T_3 (60 mg/l)	86.33	0.116	4.267	4.233	0.043
	T_4 (80 mg/l)	95.33	0.132	3.700	4.463	0.056
	T_5(100 mg/l)	90.33	0.114	3.873	4.670	0.050
Ag NPs	T_6 (5 mg/l)	80.00	0.102	4.500	4.150	0.043
	T_7 (10 mg/l)	83.33	0.114	5.343	4.147	0.047
	T_8(20 mg/l)	66.66	0.088	5.537	2.807	0.025
	T_9 (40 mg/l)	67.66	0.075	5.803	1.627	0.017
	T_{10}(60 mg/l)	62.00	0.065	6.407	1.580	0.016
SiO_2 NPs	T_{11} (5 mg/l)	86.66	0.116	4.780	3.930	0.039
	T_{12}(10 mg/l)	90.00	0.129	4.447	4.717	0.045
	T_{13}(15 mg/l)	93.33	0.130	4.640	4.427	0.045
	T_{14} (20 mg/l)	92.33	0.125	5.187	3.857	0.049
	T_{15}(50 mg/l)	86.61	0.118	5.243	3.320	0.047
	C.D. (0.05)	**13.64**	**0.004**	**0.077**	**0.073**	**0.002**
	SE(m)	**4.71**	**0.001**	**0.027**	**0.025**	**0.001**

size obtained in this study is consistent with values documented in the literature pertaining to green-synthesized TiO_2 [87].

3.2.3. SEM and EDX analysis of TiO_2NP

Fig. 7c displays the scanning electron microscopy (SEM) images of the synthesized titanium dioxide (TiO_2) nanoparticles (NPs), which exhibit a spherical morphology. Research indicates that this structure is typical of metal oxides, with an average grain size of 32–55 nm [88]. Energy dispersive spectroscopy (EDS) was employed for a preliminary chemical composition analysis, as shown in Fig. 7d. The EDS spectrum, represented in green, confirms the presence of titanium (Ti) and oxygen (O), with a notably high ratio of titanium to oxygen. Three prominent peaks in the spectrum correspond to titanium and oxide molecules, offering valuable insights into the atomic percentage and mass of the TiO_2 NPs [89]. Hibiscus extract acts as a capping agent. The analysis of surface morphologies and microstructures demonstrates that the extract from *Caesalpinia pulcherrima* effectively functions as a stabilizing and capping agent in the biosynthesis of TiO_2 nanoparticles by Devikala et al. [90].

3.2.4. DLS and zeta analysis of TiO_2NP

To analyze the particle size distribution, green synthetic TiO_2 nanoparticles (NPs) underwent dynamic light scattering (DLS) analysis. The material was completely dispersed in distilled water using an ultrasonicator prior to the analysis. The results indicated that the particles were monodisperse, with an average particle size of approximately 524 nm, as shown in Fig. 10c. The stability of the nanoparticles was assessed using zeta potential measurements, which are presented in Fig. 10d. The zeta potential values were found to be highly negative, recorded at −31.7 mV, and the conductivity was measured at 0.0327 mS/cm. These values indicate good colloid stability for the particles, suggesting that they repelled each other and did not undergo flocculation. A zeta potential value within the range of ±30 mV is a crucial parameter for assessing the stability of nanoparticles [87,88,90].

3.3. Characterization of SiO_2 synthesized from Cynodon dactylon

3.3.1. FT-IR spectra of SiO_2NP

The FTIR transmission spectrum, spanning from 400 to 4000 cm^{-1}, provides clear evidence of the presence of synthesized SiO_2 nanoparticles, as illustrated in Fig. 8c. A broad peak observed between 3000 and 3700 cm^{-1} confirms the existence of O–H groups. Furthermore, peaks detected in the range of 1640 to 1500 cm^{-1} indicate the bending vibrations associated with O–H stretch bonds. Strong bands identified at 1064, 455, and 791 cm^{-1} correspond to both asymmetric and symmetric Si-O-Si stretching bonds, a conclusion that aligns with the research findings documented by Sharma et al. [100,101].

3.3.2. XRD pattern of SiO_2NP

Fig. 9c illustrates the X-ray diffraction pattern of silica nanoparticles, showing broad halo absorption bands between approximately $2\theta = 15^\circ$ and 35°, confirming their amorphous structure. The absence of sharp peaks indicates no crystalline structure in the SiO_2 nanoparticles [100]. The green-synthesized SiO_2 nanoparticles exhibit lower noise levels compared to the chemically synthesized ones. Additionally, the peaks align with the reference JCPDS file No. 89–0510 for SiO_2, confirming the absence of impurity peaks [101–103].

3.3.3. SEM and EDX of SiO_2NP

The SEM analysis results reveal that the silica nanoparticles (SiO_2 NPs) are uniformly distributed with a spherical aggregate morphology, as shown in Fig. 7e. The SEM image confirms their green coloration and characteristic structure, which prior studies of Zaheer et al. [102] suggest is typically associated with metal oxides. The average particle size of the SiO_2 nanoparticles ranges from 31.5 to 35 nm, with particle size reduction generally being inversely proportional to surface area [100,101]. Further chemical analysis conducted via Energy Dispersive Spectroscopy (EDS) is presented in Fig. 7f, revealing the primary elements of silicon (Si) and oxygen (O) in the synthesized nanoparticles. The composition shows a significant silica proportion, comparable to the oxygen content, supporting the findings of previous research [103].

3.3.4. DLS and zeta analysis of SiO_2NP

Particle size studies were conducted to evaluate the distribution of SiO_2 nanoparticles using the dynamic light scattering (DLS) technique, as shown in Fig. 10e. The analysis revealed an average particle size of 31.44 nm and a polydispersity index (PDI) of 0.484, indicating a narrow size distribution suitable for DLS evaluation, supported findings in Refs. [102,103]. The zeta potential of the SiO_2 nanoparticles was measured at −45 mV, as shown in Fig. 10f, which suggests good stability. Variations in the zeta potential are likely due to agglomeration observed in the scanning electron microscopy (SEM) analysis, a common issue associated with the green synthesis method and potentially linked to insufficient capping agents in certain plant extracts, suggested by Min et al. [104].

3.4. Induced effects of green synthesized nano particles on germination and seedling attributes of African marigold (Tagates erecta) cv. Pusa Basanti Ganda

The recent trial results indicate that treatments T_4 and T_5 achieved the highest final germination percentages, at 96.67 % and 93.33 %, respectively, associated with increased concentrations of titanium dioxide nanoparticles (TiO_2 NP). The seedlings were examined under a range of concentrations of plant-mediated nanoparticles, as illustrated in Fig. 13(a–d). This aligns with findings from Rafique et al. [106], which reported a decrease in germination percentage with higher concentrations of silver nanoparticles (SNP), as shown in Table 4. Specifically, treatment T_6 (5 mg/L) yielded 83.33 % germination, while T_{10} (60 mg/L) recorded 63.33 %. Treatment T_{13}, with

Table 5
Effects of green synthesized nanoparticles on seedling attributes of Pusa Narangi Ganda.

	TREATMENT	SHOOT LENGTH (cm)	ROOT LENGTH (cm)	TOTAL LENGTH	VIGOUR INDEX	ROOT FRESH WEIGHT (g)	SHOOT FRESH WEIGHT (g)	ROOT/ SHOOT	ROOT DRY WEIGHT (mg)	SHOOT DRY WEIGHT (mg)
	CONTROL	5.30	3.26	8.76	575.33	0.037	0.133	0.149	1.43	23.33
TiO_2	T_1 (20 mg/l)	6.30	4.30	10.46	821.33	0.050	0.253	0.177	2.53	35.66
NPs	T_2 (40 mg/l)	7.46	4.40	11.76	933.33	0.053	0.267	0.180	3.57	44.66
	T_3 (60 mg/l)	11.56	4.30	15.76	1415.33	0.080	0.39	0.193	4.67	50.33
	T_4 (80 mg/l)	12.30	4.50	16.70	1666.67	0.143	0.667	0.202	5.87	56.33
	T_5(100 mg/l)	9.73	3.33	13.30	1192.00	0.160	0.543	0.259	5.00	47.00
Ag NPs	T_6 (5 mg/l)	9.33	3.66	13.73	1119.33	0.057	0.327	0.132	3.40	28.66
	T_7 (10 mg/l)	9.50	4.13	13.30	1158.67	0.067	0.387	0.139	4.07	47.00
	T_8(20 mg/l)	9.47	4.43	13.76	937.33	0.087	0.447	0.214	4.63	40.00
	T_9 (40 mg/l)	9.66	3.53	13.20	578.00	0.083	0.473	0.136	4.57	36.33
	T_{10}(60 mg/l)	7.26	3.12	9.50	513.33	0.053	0.333	0.092	2.40	29.66
SiO_2	T_{11} (5 mg/l)	10.23	3.66	13.70	1216.00	0.060	0.36	0.115	3.93	33.00
NPs	T_{12}(10 mg/l)	10.46	4.20	14.63	1446.67	0.067	0.38	0.138	4.87	36.00
	T_{13}(15 mg/l)	10.66	4.26	14.76	1476.67	0.093	0.453	0.155	5.57	39.33
	T_{14} (20 mg/l)	9.60	4.30	14.13	1253.33	0.083	0.44	0.149	3.53	33.66
	T_{15}(50 mg/l)	8.33	4.60	12.63	1162.00	0.047	0.373	0.123	3.73	29.66
	C.D. (0.05)	**0.33**	**0.30**	**0.20**	**2.77**	**0.058**	**0.091**	**0.054**	**0.02**	**0.014**
	SE(m)	**0.11**	**0.10**	**9.98**	**0.95**	**0.020**	**0.031**	**0.019**	**0.02**	**0.005**

Table 6
Effects of green synthesized nanoparticles on germination attributes of Pusa Basanti Ganda.

	Treatment	FINAL GERMINATION %	GERMINATION RATE INDEX (%/day)	MEAN GERMINATION TIME (days)	COEFFICIENT OF VELOCITY	MEAN GERMINATION RATE
	CONTROL	56.67	0.084	6.180	2.76	0.027
TiO_2 NPs	T_1 (20 mg/L)	73.33	0.102	4.600	2.86	0.028
	T_2 (40 mg/L)	83.33	0.102	4.647	2.95	0.028
	T_3 (60 mg/L)	83.33	0.116	4.153	3.98	0.043
	T_4 (80 mg/L)	96.67	0.129	3.000	4.22	0.045
	T_5(100 mg/L)	93.33	0.114	3.453	4.57	0.045
Ag NPs	T_6 (5 mg/L)	83.33	0.102	4.500	4.42	0.042
	T_7 (10 mg/L)	83.33	0.114	4.660	5.14	0.052
	T_8 (20 mg/L)	73.33	0.088	4.883	2.80	0.028
	T_9 (40 mg/L)	56.67	0.075	4.503	1.62	0.017
	T_{10}(60 mg/L)	63.33	0.065	5.407	1.36	0.013
SiO_2 NPs	T_{11} (5 mg/L)	86.67	0.116	4.780	3.93	0.038
	T_{12}(10 mg/L)	86.67	0.123	4.647	4.71	0.046
	T_{13}(15 mg/L)	93.33	0.122	4.440	4.42	0.043
	T_{14} (20 mg/L)	90.00	0.121	3.667	4.85	0.047
	T_{15}(50 mg/L)	86.67	0.128	4.417	5.54	0.054
	C.D.	**13.70**	**0.003**	**0.077**	**0.30**	**0.002**
	SE(m)	**4.714**	**0.01**	**0.027**	**0.13**	**0.001**

Table 7
Effects of green synthesized nanoparticles on seedling attributes of Pusa Basanti Ganda.

	Treatment	SHOOT LENGTH (cm)	ROOT LENGTH (cm)	TOTAL LENGTH (cm)	VIGOUR INDEX	ROOT FRESH WEIGHT (gm)	SHOOT FRESH WEIGHT (gm)	ROOT/ SHOOT	ROOT DRY WEIGHT (gm)	SHOOT DRY WEIGHT (gm)
	CONTROL	4.83	3.50	8.33	609.33	0.023	0.147	0.145	0.001	0.022
TiO_2 NPs	T_1 (20 mg/L)	5.90	4.30	10.20	822.33	0.043	0.237	0.174	0.002	0.032
	T_2 (40 mg/L)	7.00	4.40	11.40	936.67	0.053	0.247	0.202	0.003	0.043
	T_3 (60 mg/L)	10.17	4.30	14.47	1420.30	0.063	0.367	0.165	0.004	0.046
	T_4 (80 mg/L)	11.80	4.67	16.47	1649.30	0.127	0.620	0.193	0.006	0.052
	T_5(100 mg/L)	10.43	4.70	15.13	1177.30	0.147	0.530	0.264	0.005	0.044
Ag NPs	T_6 (5 mg/L)	9.46	3.73	13.20	1104.70	0.047	0.317	0.127	0.003	0.023
	T_7 (10 mg/L)	9.93	4.10	14.03	1187.30	0.057	0.413	0.135	0.004	0.033
	T_8(20 mg/L)	9.06	4.23	13.30	956.67	0.083	0.427	0.193	0.004	0.036
	T_9 (40 mg/L)	9.20	3.53	12.73	779.33	0.067	0.520	0.132	0.004	0.042
	T_{10}(60 mg/L)	6.80	3.23	10.03	521.67	0.033	0.347	0.088	0.002	0.032
SiO_2 NPs	T_{11} (5 mg/L)	9.20	3.67	12.87	1224.70	0.04	0.320	0.097	0.003	0.027
	T_{12}(10 mg/L)	9.66	4.20	13.87	1470.70	0.043	0.330	0.126	0.004	0.029
	T_{13}(15 mg/L)	9.83	4.27	14.10	1474.30	0.067	0.437	0.138	0.005	0.035
	T_{14} (20 mg/L)	10.20	4.30	14.50	1261.30	0.07	0.413	0.122	0.003	0.037
	T_{15}(50 mg/L)	10.60	4.73	15.33	1136.30	0.103	0.407	0.161	0.003	0.028
	C.D.	**1.88**	**0.68**	**2.04**	**2.77**	**0.016**	**0.05**	**0.003**	**0.001**	**0.003**
	SE(m)	**0.65**	**0.34**	**0.70**	**7.35**	**0.006**	**0.01**	**0.001**	**0.002**	**0.001**

15 mg/L of silica nanoparticles (SiO_2 NP), demonstrated the highest germination percentage. The Germination Rate Index (GRI) was highest for T_4 and T_5 at 0.129 and 0.114, respectively. Seeds treated with silver nanoparticles took longer to germinate, with times ranging from 4.5 to 5.40 days; T_6 recorded the shortest mean germination time (MGT) at 4.5 days, compared to T_{10}, which had the longest at 5.40 days. The control group (T_0) recorded the lowest cumulative germination value (CVG) at 2.76. In TiO_2 NP treatments, increasing concentration resulted in higher CVG values [29,32,33]. For SNPs, T_{10} had the lowest CVG at 1.36, while T_7 showed a value of 5.14. The mean germination rate (MGR) was lowest in T_{10} for SNPs at 0.013 and highest in T_{15} at 0.054 [34,36,38]. Subsequent to an examination of germination parameters, the seedling parameters were evaluated under standardized laboratory conditions. The maximum shoot length was recorded in the Titanium Dioxide-treated plate T_4 at 11.80 cm, while the control group (T_0) measured 4.83 cm [106,107]. In the third segment of the pro tray experiment with Silica Oxide nanoparticles (NPs), T_{14} and T_{15} showed the highest shoot lengths of 10.20 cm and 10.60 cm, respectively. For root length, T_4 again recorded the maximum at 4.70 cm, whereas the minimum was in control T_{10} at 3.23 cm. Control T_0 measured 3.50 cm. In Silver NPs, T_7 and T_8 exhibited favourable root lengths of 4.10 cm and 4.23 cm, respectively (see Table 5). Total length, calculated by summing shoot and root lengths, was lowest in control T_0 at 8.33 cm, supported by Farahi et al. [105]. Within the Titanium Dioxide trial, T_4 achieved the highest total length of 16.47 cm. The Vigor Index (VI), which reflects seedling health, was lowest in T_{10} at 521.67 for Silver NPs, comparable to 609.33 for control T_0. This index was acceptable for both TiO_2 and SiO_2 NPs, due to the mobilization of soluble sugars during seed germination and early seedling growth [106]. In the pro tray experiment with Silica Oxide NPs, T_{15} had the highest root fresh weight (RFW) at 0.103 g, followed by T_{14} at 0.07 g. With Titanium Dioxide NPs, T_2 and T_4 had favourable ratios of 0.202 and 0.193, respectively. Among T_6 to T_{10} with Silver NPs, T_{10} had the lowest values, while T_8 showed a better ratio of 0.193, supported by Almutairi and Alharbi [108]. Shoot dry weight, measured in grams (also expressible in milligrams), was negligible, with control T_0 showing the lowest at 0.022 g (22 mg), followed by T_6 at 0.023 g (23 mg).

3.5. *Induced effects of green synthesized nano particles on germination and seedling attributes of African marigold (Tagates erecta) cv. Pusa Narangi Ganda*

The trial results demonstrate that treatments T_4 and T_5 achieved the highest final germination percentages at 95.33 % and 90.33 %, respectively, with increased concentrations of titanium dioxide nanoparticles (TiO_2 NP) [33,34]. Treatment T_6 (5 mg/L) exhibited an 80.00 % germination rate, while T_{10} (60 mg/L) resulted in 62.00 %. In contrast, treatment T_{15} (50 mg/L of silica nanoparticles, SiO_2 NP) showed the lowest germination percentage at 86.61 %. Treatments T_{13} and T_{14}, with 15 mg/L and 20 mg/L of SiO_2 NP, demonstrated acceptable percentages of 93.33 % and 92.33 % (see Table 6). SiO_2 NP performance paralleled that of TiO_2 NP, with the highest germination rate index (GRI) of 0.130 in T_{13}. Silver nanoparticle-treated seeds required longer germination times, ranging from 4.5 to 6.4 days. For SiO_2 NP, the mean germination time (MGT) varied from 4.6 to 5.2 days, with T_{12} recording the shortest at 4.40 days. The control group (T_0) had the lowest coefficient of variation in germination (CVG) at 2.76. Similarly, SiO_2 NP exhibited CVG values from 3.32 to 4.71, with T_{12} recording the highest at 4.71. The mean germination rate (MGR) was lowest in T_{10} for silver nanoparticles at 0.016 and highest in T_4 at 0.056, consistent with findings by Carbone et al. [111] regarding seed germination influenced by plant hormones enhanced by nanoparticles. Recent observations indicate that shoot length was maximally recorded in the Titanium dioxide-treated plate T_4 at 12.30 cm and minimally in the control group T_0 at 5.30 cm. In the Silver nanoparticles (NPs) treatment, T_{10} exhibited the lowest shoot length at 7.26 cm, suggesting that higher concentrations of silver NPs may negatively affect growth parameters similar to germination effects. In the pro-tray trial involving Silica Oxide NPs, treatments T_{14} and T_{15} recorded the highest root lengths at 4.30 cm and 4.60 cm, respectively, likely due to rapid metabolic reactions initiated by the nanoparticles, findings were supported by Rehman et al. [110]. Table 7 illustrates the Vigor Index (VI), which indicates seedling health. The lowest VI was found in the silver NPs treatment T_{10} at 513.33, compared to 575.33 in the control group T_0 (Fig. 13 b). Notably, Titanium dioxide treatment T_4 achieved the highest VI at 1666.67, followed by T_3 and T_5 at 1415.33 and 1192.00, respectively [29]. For Shoot Fresh Weight (SFW), the maximum was observed in Titanium dioxide-treated tray T_4 at 0.667 g, while the control group T_0 recorded a minimum of 0.133 g. The Shoot Dry Weight (SDW) values were minimal, with T_0 recording the lowest at 0.023 g (23.33 mg), followed by T_6 at 28 mg. Overall, these findings suggest that nanoparticles enhance cell division and increase the activity of enzyme nitrate reductase, thereby promoting root development, suggested by Acharya et al. [109].

3.6. *Correlation matric analysis*

The simple correlation coefficients between conc. NPs and various germination and seedling attributes of Pusa Basanti Ganda and Pusa Narangi Ganda were computed and they are presented in Figure. The results obtained through the correlation coefficients indicate a strong association between seed morphological characters with conc. of nano salt. A positive correlation between desirable characters is favourable to the researchers which helps in simultaneous improvement of the characters and further study the interaction among the salt's concentration. It has been accounted that final germination % of Pusa Narangi Ganda (PNG) was positively linked with GRI (0.810) at $p = 0.01$, at the same time negatively linked with mean germination time (MGT) with the value of (−0.535). Total length is positively associated with shoot length (0.993), vigour index (0.992) at $p = 0.01$. Root length of PNG is significantly associated with shoot dry weight (0.485) at 5 % level of significance (Fig. 12a and b). Root/shoot ratio is significantly positively associated with shoot dry weight (0.501) at $p = 0.05$ with significance value of 0.034. In the aspects of (PBG) Pusa Basanti Ganda Final, germination % is positively correlated with GRI, MGR and COV with the values 0.866, 0.756 and 0.743 respectively at $p = 0.01$.

Research findings were supported by previous works of Doğan et al. [103], demonstrated that silica nanoparticles improve seed germination in tomato plants. Increased percentage of soybean germination by combining nanoparticles of silicon and titanium has

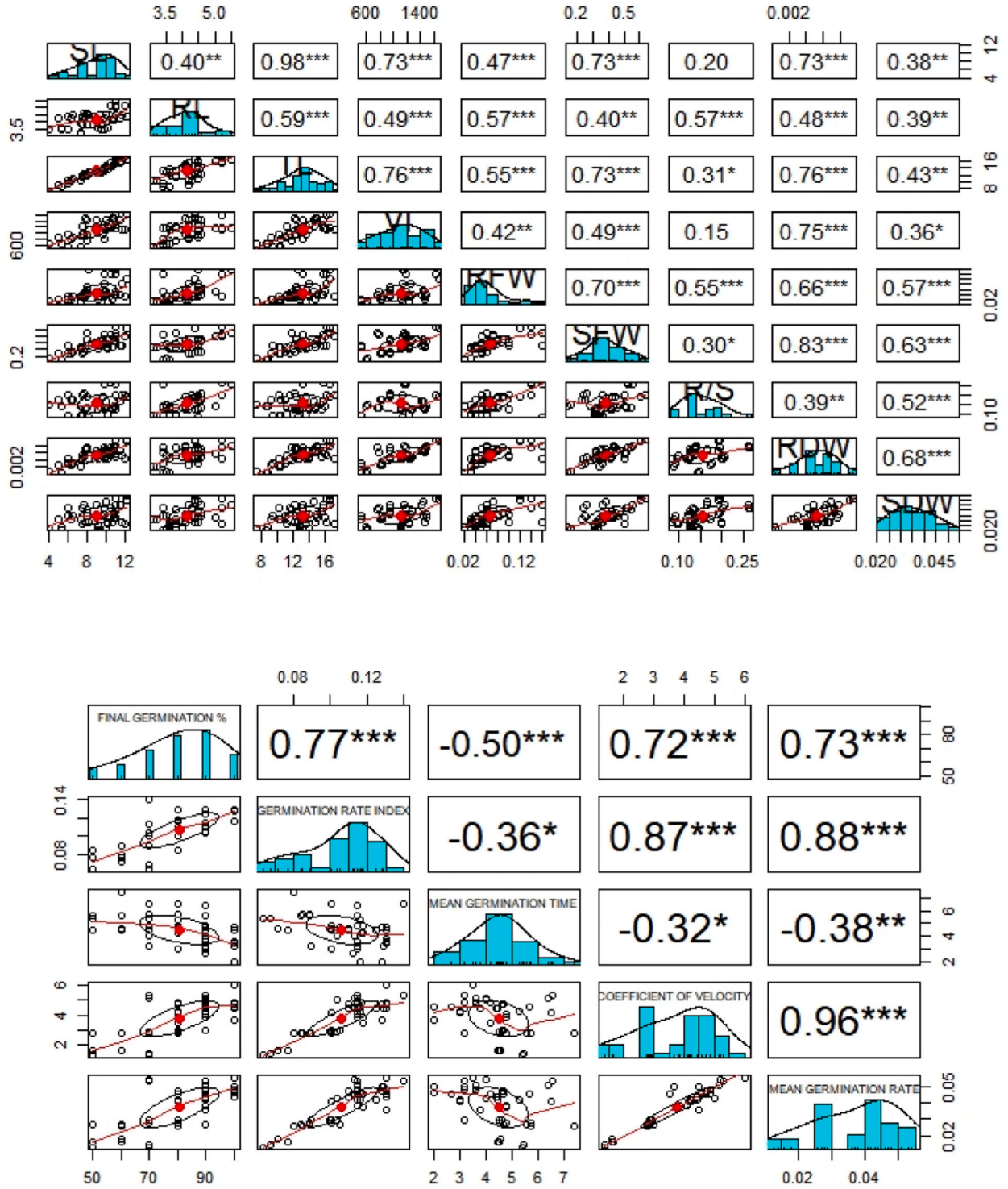

Fig. 11. Correlations Metrix of (a) Seedling attributes (b) Germination attributes of Pusa Basanti Ganda.

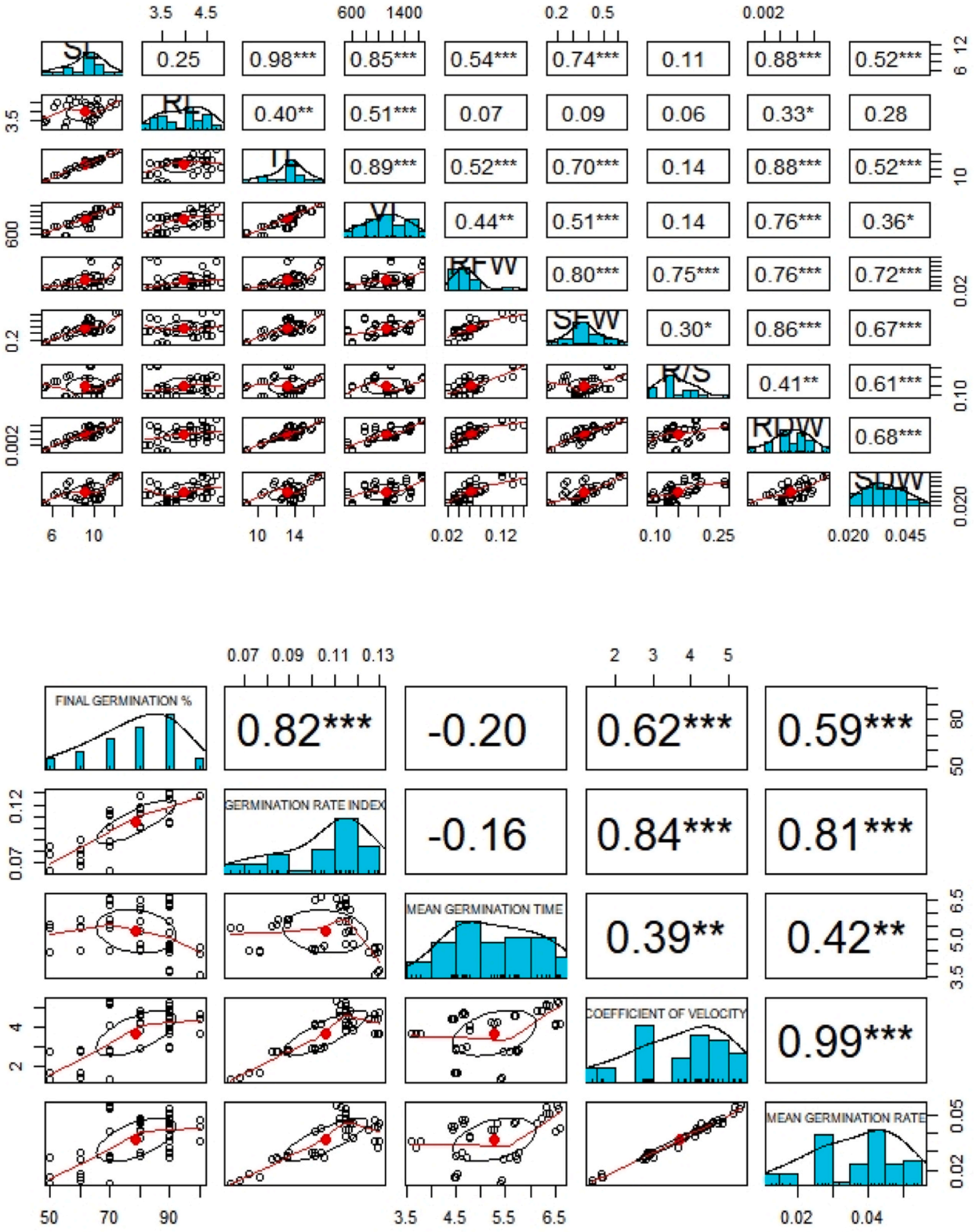

Fig. 12. Correlations Metrix of (a) Seedling attributes (b) Germination attributes of Pusa Narangi Ganda.

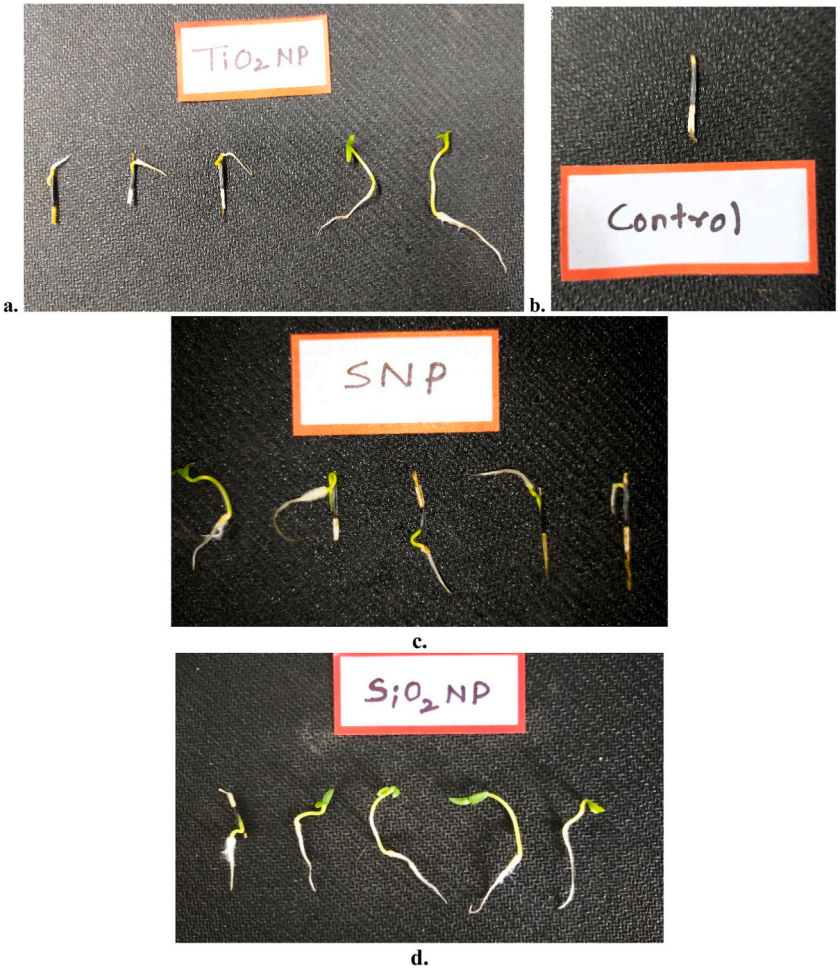

Fig. 13. a. The effect of different concentrations of TiO_2 nanoparticles on African marigold seedlings. b. Seed without treatment (Control) c. Seedling growth of seeds treated with silver nanoparticles was restricted at high concentrations (40–60 ppm). d. Healthy marigold seedlings treated with various concentrations of SiO_2 nanoparticles showed improved growth quality with increasing concentration (5–50 ppm).

also been observed [105,106] this study, the addition of silicon to form sodium silicate and silica nanoparticles become improves seed germination. In PBG, Coefficient of velocity of germination (COV) is positively correlated with FG, GRI & MGR with the value of 0.743, 0.789 and 0.851 respectively at 1 % level of significance (Fig. 11a b)) [19,20]. Vigour index is positively correlated with shoot length (0.779), root length (0.602) and root dry weight (0.601) at $p = 0.01$ as shown in Figure. From the correlation matrix it has been observed that SNPs have some deleterious effects over the germination and seedling attributes of PBG, this finding were supported by some previous research work stated by Mokula and Husen [112], that the uptake of Ag NPs by the roots was clearly exhibited, moreover, Ag NP toxicity was shown to be size and concentration dependent. While 80 nm-sized Ag NPs were only deteriorative at higher doses, those of 20 and 40 nm caused severe growth inhibition of the root [112].

4. Conclusion

Research indicates that ornamental plants can effectively synthesize nanoparticles, with phytochemicals acting as capping, reducing, and stabilizing agents. Characterization of these biologically synthesized nanoparticles shows suitable sizes for seed treatment and foliar application, along with good stability. Titanium dioxide nanoparticles at high concentrations yield the best results, while silver nanoparticles inhibit germination and negatively affect seedling growth. Silica nanoparticles, being amorphous, demonstrate positive effects at moderate concentrations but harmful impacts at high levels. Further studies are necessary to explore the influence of nanoparticles on marigold's vegetative and flowering traits. Additionally, recommending standardized doses of nanomaterials to farmers could enhance crop production and improve yield quality.

Data will be made available on request. For requesting data, please write to the corresponding author.

CRediT authorship contribution statement

Kunal Adhikary: Writing – review & editing, Writing – original draft, Resources, Methodology, Investigation, Data curation, Conceptualization. **Tapas Mondal:** Supervision, Methodology. **Jayoti Majumder:** Validation, Supervision, Resources. **Tapas Kumar Chowdhuri:** Supervision, Conceptualization. **Subhra Mukherjee:** Visualization, Validation, Supervision, Conceptualization. **Karishma Maherukh:** Writing – review & editing.

Declaration of competing interest

The authors declare that they have no known competing financial interests or personal relationships that could have appeared to influence the work reported in this paper.

References

[1] N. Kaushik, M.S. Thakkar, S. Snehit, M.S. Mhatre, Y. Rasesh, M.S. Parikh, Biological synthesis of metallic nanoparticles, Nanomed. Nanotechnol. Biol. Med. 6 (2010) 257–262.
[2] X.W. Wang, L. Zhang, C.L. Ma, R.Y. Song, H.B. Hou, D.L. Li, Enrichment and separation of silver from waste solutions by metal ion imprinted membrane, Hydrometal 100 (2009) 82–86.
[3] J. Gokulakrishnan, K. Elumalai, P. Surya, M. Baranitharan, K. Rajaganesh, H. Irrusappan, A. Kudamba, Tinospora malabarica leaf extract fractions-derived silver nanoparticles and their spectral characterisation: evaluation of their toxicity properties against agricultural pests *Spodoptera litura* and *Helicoverpa armigera*, Mater. Technol. 39 (1) (2024) 236122.
[4] K. Seku, S.S. Hussaini, G.B. Reddy, M.R.K. Reddy, Silver-based bio fungicides for the suppression of pathogenic fungi in agriculture fields, in: Nanofungicides, 2024, pp. 169–194.
[5] V.P. Zharov, J.W. Kim, D.T. Curiel, M. Everts, Self-assembling nanoclusters in living systems: application for integrated photothermal nanodiagnostics and nanotherapy, Nanomed. Nanotechnol. Biol. Med. 1 (4) (2005) 326–345.
[6] T. Santhoshkumar, R.K. Govindarajan, C. Kamaraj, C. Ragavendran, M.A. Kamal, E.H. Moglad, K.H. Baek, Green fabricated silver nanoparticles as a new eco-friendly insecticide for controlling stored cowpea bug *Callosobruchus maculatus* (Coleoptera: bruchidae), Biocatal. Agric. Biotechnol. 56 (2024) 103023.
[7] A. Khan, A. Raza, A. Hashem, G. Dolores Avila-Quezada, E. Fathi Abd_Allah, F. Ahmad, A. Ahmad, Green fabrication of titanium dioxide nanoparticles via *Syzygium cumini* leaves extract: characterizations, photocatalytic activity and nematicidal evaluation, Green Chem. Lett. Rev. 17 (1) (2024) 2331063.
[8] A.M. Ahmed, K.A. Khalid, F.S. Zaki, Investigating foliar application of bulk and nanoparticles titanium dioxide on fennel productivity to mitigate the negative effects of saline irrigation water, BMC Plant Biol. 24 (1) (2024) 317.
[9] S. Ali, R.A. Mir, A. Tyagi, N. Manzar, A.S. Kashyap, M. Mushtaq, H. Bae, Chromium toxicity in plants: signaling, mitigation, and future perspectives, Plants 12 (7) (2023) 1502.
[10] G. Mustafa, S. Komatsu, Plant proteomic research for improvement of food crops under stresses: a review, Molecular omics 17 (6) (2021) 860–880.
[11] Y. Abdelkader, L. Perez-Davalos, R. LeDuc, R.P. Zahedi, H.I. Labouta, Omics approaches for the assessment of biological responses to nanoparticles, Adv. Drug Deliv. Rev. (2023) 114992.
[12] S. Abedini, S. Pourseyedi, J. Zolala, H. Mohammadi, R. Abdolshahi, Green synthesis of superparamagnetic iron oxide and silver nanoparticles in satureja hortensis leave extract: evaluation of antifungal effects on botryosphaeriaceae species, Curr. Microbiol. 81 (6) (2024) 149.
[13] P. Tundo, P. Anastas, D.S. Black, J. Breen, T.J. Collins, S. Memoli, W. Tumas, Synthetic pathways and processes in green chemistry. Introductory overview, Pure Appl. Chem. 72 (7) (2000) 1207–1228.
[14] S.M. Reed, J.E. Hutchison, Green chemistry in the organic teaching laboratory: an environmentally benign synthesis of adipic acid, J. Chem. Educ. 77 (12) (2000) 1627.
[15] S.I.U. Haq, S. Wali, N.U. Sama, K. Kamran, Z. Ullah, H.I. Mohamed, Environmentally friendly synthesis of silver nanoparticles (AgNPs) using mentha arvensis plants modulates physiological and biochemical attributes and yield of sunflower (*Helianthus annuus* L.), J. Soil Sci. Plant Nutr. (2024) 1–21.
[16] S.Y. Park, S.P. Murphy, L.R. Wilkens, B.E. Henderson, L.N. Kolonel, Multivitamin use and the risk of mortality and cancer incidence: the multiethnic cohort study, Am. J. Epidemiol. 173 (2011) 906–914.
[17] P. Raveendran, J. Fu, S.L. Wallen, Completely "green" synthesis and stabilization of metal nanoparticles, J. Am. Chem. Soc. 125 (2003) 13940–13941.
[18] T. Guha, K.V.G. Ravikumar, A. Mukherjee, A. Mukherjee, R. Kundu, Nanopriming with zero valent iron (nZVI) enhances germination and growth in aromatic rice cultivar (*Oryza sativa* cv. Gobindabhog L.), Plant Physiol. Biochem. 127 (2018) 403–413.
[19] U. Chandrasekaran, X. Luo, Q. Wang, K. Shu, Are there unidentified factors involved in the germination of nano primed seeds? Front. Plant Sci. 11 (2020) 832.
[20] A. Joshi, S. Kaur, K. Dharamvir, H. Nayyar, G. Verma, Multi-walled carbon nanotubes applied through seed-priming influence early germination, root hair, growth and yield of bread wheat (*Triticum aestivum* L.), J. Sci. Food Agric. 98 (8) (2018) 3148–3160.
[21] X.Y. Ji, H.Y. Wang, B. Song, B.B. Chu, Y. He, Silicon nanomaterials for biosensing and bioimaging analysis, Front. Chem. 6 (2018).
[22] L. Mahawar, K.P. Ramasamy, M. Suhel, S.M. Prasad, M. Zivcak, M. Brestic, et al., Silicon nanoparticles: comprehensive review on biogenic synthesis and applications in agriculture, Environ. Res. 232 (2023) 116292.
[23] K. Bansal, V. Hooda, N. Verma, T. Kharewal, N. Tehri, V. Dhull, et al., Stress alleviation and crop improvement using silicon nanoparticles in agriculture: a review, Silicon 14 (2022) 10173–10186.
[24] K.K. Verma, Y. Zeng, X.P. Song, M. Singh, K.C. Wu, V.D. Rajput, et al., Nanosilicon: an approach for abiotic stress mitigation and sustainable agriculture, Front. Plant Sci. 13 (2022) 1025974.
[25] L. Wang, C. Ning, T. Pan, K. Cai, Role of silica nanoparticles in abiotic and biotic stress tolerance in plants: a review, Int. J. Mol. Sci. 23 (2022) 1947.
[26] P. Mathur, S. Roy, Nanosilica facilitates silica uptake, growth and stress tolerance in plants, Plant Physiol. Biochem. 157 (2020) 114–127.
[27] J. Zhang, S. Kothalawala, C.Z. Yu, Engineered silica nanomaterials in pesticide delivery: challenges and perspectives, Environ. Pollut. 320 (2023) 14.
[28] S. Sagadevan, S. Imteyaz, B. Murugan, J.A. Lett, N. Sridewi, G.K. Weldegebrieal, et al., A comprehensive review on green synthesis of titanium dioxide nanoparticles and their diverse biomedical applications, Green Process, Synth. Met. 11 (1) (2022) 44–63.
[29] C.P. Andersen, G. King, M. Plocher, M. Storm, L.R. Pokhrel, M.G. Johnson, et al., Germination and early plant development of ten plant species exposed to titanium dioxide and cerium oxide nanoparticles, Environ. Toxicol. Chem. 35 (9) (2016) 2223–2229.
[30] H. Kiapour, P. Moaveni, D. Habibi, Evaluation of the application of gibbrellic acid and titanium dioxide nanoparticles under drought stress on some traits of basil (*Ocimum basilicum* L.), Int. J. Agron. Agric (2015) 138–150.
[31] K.S. Siddiqi, A. Husen, Plant response to engineered metal oxide nanoparticles, Nanoscale Res. Lett. 12 (1) (2017) 92.
[32] R.G. Saratale, I. Karuppusamy, G.D. Saratale, A. Pugazhendhi, G. Kumar, Y. Park, et al., A comprehensive review on green nanomaterials using biological systems: recent perception and their future applications, Colloids Surf. B Biointerfaces 170 (2018) 20–35.
[33] A. Sivakami, R. Sarankumar, S. Vinodha, Introduction to nanobiotechnology: novel and smart applications, Bio-manufactured Nanomaterials: Perspect. Promotion (2021) 1–22.
[34] A. Tripathy, A.M. Raichur, N. Chandrasekaran, T.C. Prathna, A. Mukherjee, Process variables in biomimetic synthesis of silver nanoparticles by aqueous extract of *Azadirachta indica* (Neem) leaves, J. Nanoparticle Res. 12 (1) (2010) 237–246.

[35] M. Snoussi, R.H. Lajimi, S. Latif, W.S. Hamadou, M. Alreshidi, S.A. Ashraf, M. Patel, J.R. Humaidi, A. Kadri, E. Noumi, Green synthesis and characterization of silver nanoparticles from *Ducrosia flabellifolia* Boiss. aqueous extract: anti-quorum sensing screening and antimicrobial activities against ESKAPE pathogens, Cell. Mol. Biol. 70 (2) (2024) 88–96.

[36] R. Kini, R. Trivedi, M.H. Mujahid, P. Patra, S.A. Alharbi, F.D. Alshammari, M.B. Bealy, A.E.O. Elkhalifa, S. Siddiqui, T.K. Upadhyay, Green synthesis and characterization of silver nanoparticles from nerium indicum and investigation of antioxidant and anti-cancerous potential against cervical cancer cell line (HeLa), Ind. J. Pharm. Educ. Res 58 (2024) 565–578.

[37] S. Khan, M. Zahoor, R.S. Khan, M. Ikram, N.U. Islam, The impact of silver nanoparticles on the growth of plants: the agriculture applications, Heliyon 9 (6) (2023) e16928.

[38] O.M. Ali, M.S. Hasanin, W.B. Suleiman, E.E.H. Helal, A.H. Hashem, Green biosynthesis of titanium dioxide quantum dots using watermelon peel waste: antimicrobial, antioxidant, and anticancer activities, Biomass Conversion and Biorefinery 14 (5) (2024) 6987–6998.

[39] National horticulture Board's (NHB). https://www.apeda.gov.in/apedawebsite/SubHead_Products/Floriculture.htm. (Accessed 6 November 2024).

[40] J. Kangsopa, A. Singsopa, N. Thawong, Marigold seed pelleting with plant nutrients on germination, growth, storage and flower yields, Indian J. Agric. Res. 1 (2023) 7.

[41] J. Srichok, N. Yingbun, T. Kowawisetsut, S. Kornmatitsuk, U. Suttisansanee, P. Temviriyanukul, B. Chantong, Synergistic antibacterial and anti-inflammatory activities of *Ocimum tenuiflorum* ethanolic extract against major bacterial mastitis pathogens, Antibiotics 11 (2022) 510.

[42] A.M. Alex, S. Subburaman, S. Chauhan, V. Ahuja, G. Abdi, M.A. Tarighat, Green synthesis of silver nanoparticle prepared with Ocimum species and assessment of anticancer potential, Sci. Rep. 14 (1) (2024) 11707.

[43] G. Singhal, R. Bhavesh, K. Kasariya, A.R. Sharma, R.P. Singh, Biosynthesis of silver nanoparticles using *Ocimum sanctum* (Tulsi) leaf extract and screening its antimicrobial activity, J. Nanoparticle Res. 13 (2011) 2981–2988.

[44] B.S. Prathibha, N. Harshitha, D.R. Neha, C.N. Pranathi, D.V. Kumar, G.C. Lakshmi, Green synthesis of silver nanoparticles using *Ocimum tenuiflorum* and *Azadirachta indica* leaf extract and their antibacterial activity, J. Phys. Conf. 2748 (1) (2024, April) 012015. IOP Publishing.

[45] F. Atmani, C. Sadki, M. Aziz, M. Mimouni, B. Hacht, *Cynodon dactylon* extract as a preventive and curative agent in experimentally induced nephrolithiasis, Urol. Res. 37 (2009) 75–82.

[46] R.H. Babu, P. Yugandhar, N. Savithramma, Synthesis, characterization and antimicrobial studies of bio silica nanoparticles prepared from *Cynodon dactylon* L.: a green approach, Bull. Mater. Sci. 41 (2018) 1–8.

[47] A. Tiwari, K. Pandey, S. Singh, S. Chawla, Grass and their waste products for nanoparticles synthesis and applications, in: Nanomaterials from Agricultural and Horticultural Products, Springer Nature Singapore, Singapore, 2023, pp. 261–271.

[48] D. Vishnu, B. Dhandapani, Integration of *Cynodon dactylon* and *Muraya koenigii* plant extracts in amino-functionalised silica-coated magnetic nanoparticle as an effective sorbent for the removal of chromium (VI) metal pollutants, IET Nanobiotechnol. 14 (6) (2020) 449–456.

[49] S.A.I.M. Sopi, M.H.A. Hassan, A review on the extraction of silica nanoparticles from poaceae family via sol-gel, Malaysian Journal of Science Health & Technology 10 (1) (2024) 7–18.

[50] G.O. Ostapchuk, Eco-friendly synthesis of silica nanoparticles and their applications, Materials Research Foundations (2024) 169.

[51] S. Rengarajan, V. Melanathuru, C. Govindasamy, V. Chinnadurai, M.F. Elsadek, Antioxidant activity of flavonoid compounds isolated from the petals of Hibiscus rosa sinensis, J. King Saud Univ. Sci. 32 (3) (2020) 2236–2242.

[52] K.G. Rao, C.H. Ashok, K.V. Rao, C.S. Chakra, V. Rajendar, Green synthesis of TiO_2 nanoparticles using hibiscus flower extract, in: Proceedings of the International Conference on Emerging Technologies in Mechanical Sciences, 2014, December, pp. 79–82.

[53] M.F.H. Abd El-Kader, M.T. Elabbasy, A.A. Adeboye, M.G. Zeariya, A.A. Menazea, Morphological, structural and antibacterial behavior of eco-friendly of ZnO/TiO_2 nanocomposite synthesized via *Hibiscus rosa-sinensis* extract, J. Mater. Res. Technol. 15 (2021) 2213–2220.

[54] M. Kaur, J. Singh, M. Chauhan, V. Kumar, K. Singh, Green synthesis of TiO_2-Al_2O_3-$ZnFe_2O_4$ nanocomposite using the *Hibiscus rosa sinesis* and evaluation of its photocatalytic applications, Open Ceramics 18 (2024) 100571.

[55] D.R. Eddy, D. Rahmawati, M.D. Permana, T. Takei, A.R. Noviyanti, I. Rahayu, A review of recent developments in green synthesis of TiO_2 nanoparticles using plant extract: synthesis, characterization and photocatalytic activity, Inorg. Chem. Commun. (2024) 112531.

[56] J.D. Clogston, R.M. Crist, M.A. Dobrovolskaia, S.T. Stern (Eds.), Characterization of Nanoparticles Intended for Drug Delivery, Humana Press, 2024, pp. 63–70.

[57] X.Q. Zhou, Z. Hayat, D.D. Zhang, M.Y. Li, S. Hu, Q. Wu, Y. Yuan, Zinc oxide nanoparticles: synthesis, characterization, modification, and applications in food and agriculture, Processes 11 (4) (2023) 1193.

[58] G. Magdy, E. Aboelkassim, S.M. Abd Elhaleem, F. Belal, A comprehensive review on silver nanoparticles: synthesis approaches, characterization techniques, and recent pharmaceutical, environmental, and antimicrobial applications, Microchem. J. 196 (2024) 109615.

[59] C. Hano, B.H. Abbasi, Plant-based green synthesis of nanoparticles: production, characterization and applications, Biomolecules 12 (1) (2021) 31.

[60] K.U. Tümen, B. Kıvrak, F.Ö. Alkurt, M. Akyol, M. Karaaslan, A. Ekicibil, Synthesis and characterization of nanoparticles reinforced epoxy based advanced radar absorbing composites, J. Mater. Sci. Mater. Electron. 32 (2021) 28007–28018.

[61] R. Jha, R.A. Mayanovic, A review of the preparation, characterization, and applications of chitosan nanoparticles in nanomedicine, Nanomaterials 13 (8) (2023) 1302.

[62] T.A. Mughal, S. Ali, S. Mumtaz, M. Summer, M.Z. Saleem, A. Hassan, M.U. Hameed, Evaluating the biological (antidiabetic) potential of TEM, FTIR, XRD, and UV-spectra observed berberis lyceum conjugated silver nanoparticles, Microsc. Res. Tech. 87 (6) (2024) 1286–1305.

[63] H. Guo, Y. Liu, J. Chen, Y. Zhu, Z. Zhang, The effects of several metal nanoparticles on seed germination and seedling growth: a meta-analysis, Coatings 12 (2) (2022) 183.

[64] A. Ali Naghizadeh, M.M. Zarandi, S.M.R. Khoshroo, F.H. Davarani, Investigating the effect of green silver nanoparticles on seed germination and physiological parameters of spinach (Spinacia oleracea L.) under salt stress, Russ. J. Plant Physiol. 71 (4) (2024) 102.

[65] G. Wang, Y. Kang, X. Li, L. Zhang, G. Xu, Y. Zheng, Effects of seed coating and priming with exogenous brassinosteroid on tobacco seed germination, J. Plant Interact. 19 (1) (2024) 2299546.

[66] Y.A. El-Kassaby, I. Moss, D. Kolotelo, M. Stoehr, Seed germination: mathematical representation and parameters extraction, For. Sci. 54 (2) (2008) 220–227.

[67] F. Kronthaler, S. Zöllner, Data analysis with RStudio. Data Analysis with RStudio, 2021.

[68] A.G. Asuero, A. Sayago, A.G. González, The correlation coefficient: an overview, Crit. Rev. Anal. Chem. 36 (1) (2006) 41–59.

[69] S. Ullah, S. Saud, K. Liu, M.T. Harrison, S. Hassan, T. Nawaz, S. Fahad, Germination response of Oat (*Avena sativa* L.) to temperature and salinity using halothermal time model, Plant Stress 10 (2023) 100263.

[70] G. Sarwar, T. Anwar, H. Qureshi, M. Younus, M.W. Hassan, M. Sajid-ur-Rehman, W. Soufan, Optimizing germination: comparative assessment of various growth media on dragon fruit germination and early growth, BMC Plant Biol. 24 (1) (2024) 533.

[71] I. Kristó, M. Vályi-Nagy, A. Rácz, K. Irmes, L. Szentpéteri, M. Jolánkai, M. Tar, Effects of nutrient supply and seed size on germination parameters and yield in the next crop year of winter wheat (*Triticum aestivum* L.), Agriculture 13 (2) (2023) 419.

[72] P. Carril, M. Ghorbani, S. Loppi, S. Celletti, Effect of biochar type, concentration and washing conditions on the germination parameters of three model crops, Plants 12 (12) (2023) 2235.

[73] S.R.G. Shiade, B. Boelt, Seed germination and seedling growth parameters in nine tall fescue varieties under salinity stress, Acta Agric. Scand. Sect. B Soil Plant Sci 70 (6) (2020) 485–494.

[74] O. Farooq, M. Ali, N. Sarwar, M. Mazhar Iqbal, T. Naz, M. Asghar, F. Ehsan, Foliar applied brassica water extract improves the seedling development of wheat and chickpea, Asian Journal of Agriculture and Biology (2021) 1.

[75] P.D. Itroutwar, G. Kasivelu, V. Raguraman, K. Malaichamy, S.K. Sevathapandian, Effects of biogenic zinc oxide nanoparticles on seed germination and seedling vigor of maize (*Zea mays*), Biocatal. Agric. Biotechnol. 29 (2020) 101778.

[76] S.A. Al-Sahli, F. Al-Otibi, R.I. Alharbi, M. Amina, N.M. Al Musayeib, Silver nanoparticles improve the fungicidal properties of Rhazya stricta decne aqueous extract against plant pathogens, Sci. Rep. 14 (1) (2024) 1297.

[77] T. Mustapha, N.R. Ithnin, H. Othman, Z.I. Abu Hasan, N. Misni, Bio-fabrication of silver nanoparticles using Citrus aurantifolia fruit peel extract (CAFPE) and the role of plant extract in the synthesis, Plants 12 (8) (2023) 1648.
[78] K. Chand, D. Cao, D.E. Fouad, A.H. Shah, A.Q. Dayo, K. Zhu, S. Dong, Green synthesis, characterization and photocatalytic application of silver nanoparticles synthesized by various plant extracts, Arab. J. Chem. 13 (11) (2020) 8248–8261.
[79] H.A. Widatalla, L.F. Yassin, A.A. Alrasheid, S.A.R. Ahmed, M.O. Widdatallah, S.H. Eltilib, A.A. Mohamed, Green synthesis of silver nanoparticles using green tea leaf extract, characterization and evaluation of antimicrobial activity, Nanoscale Adv. 4 (3) (2022) 911–915.
[80] R.B. Patil, A.D. Chougale, Analytical methods for the identification and characterization of silver nanoparticles: a brief review, Mater. Today: Proc. 47 (2021) 5520–5532.
[81] M.S. Aref, S.S. Salem, Bio-callus synthesis of silver nanoparticles, characterization, and antibacterial activities via Cinnamomum camphora callus culture, Biocatal. Agric. Biotechnol. 27 (2020) 101689.
[82] Hemlata, P.R. Meena, A.P. Singh, K.K. Tejavath, Biosynthesis of silver nanoparticles using Cucumis prophetarum aqueous leaf extract and their antibacterial and antiproliferative activity against cancer cell lines, ACS Omega 5 (10) (2020) 5520–5528.
[83] N.S. Alharbi, N.S. Alsubhi, A.I. Felimban, Green synthesis of silver nanoparticles using medicinal plants: characterization and application, Journal of Radiation Research and Applied Sciences 15 (3) (2022) 109–124.
[84] F. Rodríguez-Félix, A.G. López-Cota, M.J. Moreno-Vásquez, A.Z. Graciano-Verdugo, I.E. Quintero-Reyes, C.L. Del-Toro-Sánchez, J.A. Tapia-Hernández, Sustainable-green synthesis of silver nanoparticles using safflower (Carthamus tinctorius L.) waste extract and its antibacterial activity, Heliyon 7 (4) (2021) e06923.
[85] M. Viana, V.F.M. Soares, N.D.S. Mohallem, Synthesis and characterization of TiO_2 nanoparticles, Ceram. Int. 36 (7) (2010) 2047–2053.
[86] R. Venkatesan, T. Dhilipkumar, A. Kiruthika, N. Ali, S.C. Kim, Green composites for sustainable food packaging: exploring the influence of lignin-TiO_2 nanoparticles on poly (butylene adipate-co-terephthalate), Int. J. Biol. Macromol. 277 (2024) 134511.
[87] P. Mathumba, M.P. Bilibana, O.C. Olatunde, D.C. Onwudiwe, X-ray diffraction profile analysis of green synthesized ZnO and TiO2 nanoparticles, Mater. Res. Express 11 (7) (2024) 075011.
[88] S. Farag, A. Amr, A. El-Shafei, M.S. Asker, H.M. Ibrahim, Green synthesis of titanium dioxide nanoparticles via bacterial cellulose (BC) produced from agricultural wastes, Cellulose 28 (12) (2021) 7619–7632.
[89] K. Manimaran, S. Loganathan, D.G. Prakash, D. Natarajan, Antibacterial and anticancer potential of mycosynthesized titanium dioxide (TiO_2) nanoparticles using *Hypsizygus ulmarius*, Biomass Conversion and Biorefinery 14 (12) (2024) 13293–13301.
[90] S. Devikala, J.M. Abisharani, M. Bharath, Biosynthesis of TiO_2 nanoparticles from *Caesalpinia pulcherrima* flower extracts, Mater. Today: Proc. 40 (2021) S185–S188.
[100] P. Sharma, J. Kherb, J. Prakash, R. Kaushal, A novel and facile green synthesis of SiO_2 nanoparticles for removal of toxic water pollutants, Appl. Nanosci. 13 (1) (2023) 735–747.
[101] Y.A. Hasanien, M.A. Mosleh, A.S. Abdel-Razek, G.S. El-Sayyad, E.H. El-Hakim, E.H. Borai, Green synthesis of SiO_2 nanoparticles from Egyptian white sand using submerged and solid-state culture of fungi, Biomass Conversion and Biorefinery 14 (20) (2024) 26159–26172.
[102] S. Zaheer, J. Shehzad, S.K. Chaudhari, M. Hasan, G. Mustafa, Morphological and biochemical responses of *Vigna radiata* L. seedlings towards green synthesized SiO_2 NPs, Silicon 15 (14) (2023) 5925–5936.
[103] B. Doğan, M.K. Yeşilyurt, H. Yaman, N. Korkmaz, A. Arslan, Green synthesis of SiO_2 and TiO_2 nanoparticles using safflower (*Carthamus tinctorius* L.) leaves and investigation of their usability as alternative fuel additives for diesel-safflower oil biodiesel blends, Fuel 367 (2024) 131498.
[104] K.H. Min, J.W. Shin, M.R. Ki, S.P. Pack, Green synthesis of silver nanoparticles on biosilica diatomite: well-dispersed particle formation and reusability, Process Biochem. 125 (2023) 232–238.
[105] S.M.M. Farahi, M.E.T. Yazdi, E. Einafshar, M. Akhondi, M. Ebadi, S. Azimipour, et al., The effects of titanium dioxide (TiO_2) nanoparticles on physiological, biochemical, and antioxidant properties of Vitex plant (*Vitex agnus-Castus* L), Heliyon 9 (11) (2023) e22144.
[106] M. Rafique, J. Jahangir, B.A.Z. Amin, M. Bilal Tahir, G. Nabi, M. Isa Khan, I. Sadaf, Investigation of photocatalytic and seed germination effects of TiO_2 nanoparticles synthesized by *Melia azedarach* L. leaf extract, J. Inorg. Organomet. Polym. Mater. 29 (6) (2019) 2133–2144.
[107] N. Samadi, S. Yahyaabadi, Z. Rezayatmand, Effect of TiO_2 and TiO_2 nanoparticle on germination, root and shoot length and photosynthetic pigments of *Mentha piperita*, Int. J. Plant Soil Sci 3 (4) (2014) 408–418.
[108] Z.M. Almutairi, A. Alharbi, Effect of silver nanoparticles on seed germination of crop plants, Int. J. Nucl. Quant. Eng. 9 (6) (2015) 689–693.
[109] P. Acharya, G.K. Jayaprakasha, K.M. Crosby, J.L. Jifon, B.S. Patil, Nanoparticle-mediated seed priming improves germination, growth, yield, and quality of watermelons (*Citrullus lanatus*) at multi-locations in Texas, Sci. Rep. 10 (1) (2020) 5037.
[110] M.S. Rahman, A. Chakraborty, A. Kibria, M.J. Hossain, Effects of silver nanoparticles on seed germination and growth performance of pea (*Pisum sativum*), Plant Nano Biol. 5 (2023) 100042.
[111] M. Carbone, S. De Rossi, T. Donia, G.D. Di Marco, B. Gustavino, L. Roselli, A. Gismondi, Biostimulants promoting growth of Vicia faba L. seedlings: inulin coated ZnO nanoparticles, Chemi. Biol. Technol. Agric. 10 (1) (2023) 134.
[112] M.R. Mokula, A. Husen, Toxicity assessment of silver nanoparticles and silver ions on plant growth, in: Nanomaterials and Nanocomposites Exposures to Plants: Response, Interaction, Phytotoxicity and Defense Mechanisms, Springer Nature Singapore, Singapore, 2023, pp. 157–174.